UCLouvain

École polytechnique de Louvain

Isolated DC Microgrids: a paradigm-shifting technology allowing the implementation of renewable energy sources

Author: **Fernando COELHO**
Supervisor: **Emmanuel DE JAEGER**
Readers: **Eduardo VASQUEZ, Mark BEKEMANS**
Academic year 2019–2021
Master [120] in Electrical Engineering

Abstract

The great majority of countries have their energy generation highly dependent on fossil fuel sources, which leads to tragic effects on climate change. The characteristics of this generation were central in the development of our energy grids, that are centralized in terms of generation and have long AC transmission architectures. This thesis discusses an alternative to that reality: Isolated DC Microgrids, a group of interconnected loads and energy sources within clearly defined electrical boundaries, with a DC transmission strategy and storage units guaranteeing the reliability of the whole system.

While studying this alternative, we focused our attention on DC-DC converter, a group of devices that are responsible for adapting the voltage level of a given busbar, in order to comply with requirements within the microgrid. Given the wide range of DC-DC converters available in the market, we discussed the principle of operation and characteristics of the main ones, dividing them in two groups: non-isolated and isolated ones. A decision was made, mainly based on their efficiencies, to use Buck and Boost converters in our model.

Having decided for them, we had to find a control approach to be used and we went for cascade control, where we have two controllers working in series with each other, one aiming at controlling the voltage level in the output capacitor and the other the current in the converter's inductance. After that, a mathematical strategy was developed in order to correctly set the control parameters of both controllers, where we would define two time constants, one for each controller, and, based on that and the characteristics of the converters, define the control parameters that would guarantee their first order response, with the time constants previously defined.

Finally, a model of this Isolated DC Microgrid was developed on MATLAB/ Simulink, having two renewable energy sources, photovoltaic (PV) and wind, and using the control strategy defined to set the correct voltage levels at the load ends. These loads were grouped in what we called "houses", each having representations of very common residential loads, such as phones, computers, showers and even electrical vehicle (EV) chargers. With this model, we aimed at simulating a microgrid as close to the reality as possible and, as the results found were promising, we believe that a major argument in favour of this strategy was made.

Acknowledgements

This work would not have been possible without all the support and encouragement that I received from my family since little. They always motivated me to seek greater challenges and to pursue academic excellence and for that I am really grateful.

Throughout my academic life, I had the opportunity to work with and learn from great minds, that today I have the privileged to call my friends. Without their influence, I would not had the opportunities that I had and, definitely, would not enjoy as much as I did the journey.

I am, also, very thankful to my thesis advisor, professor Emmanuel De Jaeger, who guided and helped me, week after week, with his knowledge and experience. Also, I would like to thank all the professors that I had, both in Brazil and Belgium, as without their attention I would never be able to be where I am today.

Contents

Acronyms

RES: Renewable Energy Sources
PV: Photovoltaic
AC: Alternated Current
DC: Direct Current
GU: Generation Units
ESS: Energy Storage Systems
PCC: Point of Common Coupling
DG: Distributed Generation
CG: Centralized Generation
LCOE: Levelized Cost of Energy
MOSFET: Metal Oxide Semiconductor Field Effect Transistor
IGBT: insulated-gate bipolar transistor
EPA: Environmental Protection Agency
T&D: Transmission and distribution
MPP: Maximum Power Point
MPPT: Maximum Power Point Tracking
P&O: Perturb and Observe
SOC: State-of-charge

Nomenclature

θ: duty cycle of converter
V_s: voltage source
V_{in}: input voltage
V_{out} or V_o: output voltage
$V_{out,ripple}$: maximum allowed output voltage ripple
V_{load}: voltage on the load
V_L: inductor's voltage
$V_{L,ON}$: inductor's voltage when transistor is closed
$V_{L,OFF}$: inductor's voltage when transistor is opened
ΔI_L: variation in the inductor's current
$I_{L,avg}$: average current in the inductor
$I_{o,avg}$: average output current
$I_{L,0}$: current in the inductor at beginning of the period
$I_{L,\theta T}$: Current in the inductor when the switch is turned OFF
T: transistor's period
f_{sw} or f: frequency of switching
R: output load
r: inductor's parasitic resistance
L: inductance
C: capacitance
S or Q: switch
D: diode
I_S: current in the switch
C_{out}: output capacitor of a given circuit
$V_{out,ripple}$: Ripple in the output load given by the transistor being switched ON and OFF
i_M: magnetizing current
I_C: current in the capacitor
I_o: current in the output load
n: number of turns ratio of a transformer
V_T: voltage in the primary side of a transformer
I_D: diode's current
v_s: voltage in the secondary side of a transformer
V_{ref}: output voltage reference of a converter
K_p: proportional control constant of a controller
K_i: integral control constant of a controller
K_d: derivative control constant of a controller
$K_{p,voltage}$: proportional control constant of a voltage controller
$K_{i,voltage}$: integral control constant of a voltage controller

$K_{p,current}$: proportional control constant of a current controller
$K_{i,current}$: integral control constant of a current controller
x_1: measured inductor's current of a converter
x_2: measured capacitor's voltage of a converter
e_{x1}: error from the measured inductor's current and the reference one
$y = x^2$: auxiliary variable that represents the squared value of the output voltage of a capacitor
V_{DC}: DC voltage level (150V)
V_{bus}: voltage measured on the main busbar
$L_{control}$: addition of inductances of line and converter that will be used to set the control parameters
$r_{control}$: addition of resistances of line and inductor's parasitic resistance that will be used to set the control parameters
L_{line}: inductance of the transmission line
r_{line}: resistance of the transmission line
L_{boost}: input inductance of the Boost Converter
L_{boost}: inductor's parasitic resistance of the Boost Converter
I_{in}: current in the input of the Buck converter
I_{out}: current in the output of the Buck converter

Introduction

One of the main issues that our society is facing, nowadays, is climate change and how mankind should treat the environment in order to guarantee Earth´s sustainability. With that in mind, some of the most important world leaders gather together, earlier this year, in an virtual event, to discuss this topic and the outcomes were promising. There, they agreed that all countries should focus their resources on reducing greenhouse gas emissions and set some ambitious goals in that direction. The meeting ended up with some practical results, such as the European Union aiming at carbon neutrality by the year of 2050 [1] and the United States guaranteeing that they should reach 100% carbon pollution-free electricity by the year of 2035 [2], something that was unthinkable a couple of years ago.

With this ambition in mind, it is imperative to understand the main sources of these emissions and, accordingly to the United States Environmental Protection Agency (EPA), it is the burning of fossil fuels for electricity production and transportation [3]. Having understood this, we should focus our attention on an alternative to fossil fuels that is clean with respect to greenhouse gases and, as it is known, renewable energy sources (RES), such as photovoltaic (PV) and wind, are much less aggressive to the environment, as their emissions are significantly smaller, compared to fossil fuels [4].

Aligned with this necessity, recent technology improvements are a big argument in favour of the RES's case. Just in the last few decades, we saw a drastic increase in their energy efficiency and reduction in cost of manufacturing. One example of this is the cost per watt produced of PV modules, that went from more than 100 dollars per watt in the early 1970s, to around 0.2 dollars nowadays [5].

As the necessity of RES's expansion gets clearer, discussions arise regarding the best way of implementing them in terms of distribution, with two main options emerging: the centralized and the decentralized way. The first one is constituted of big generation facilities and complex grids to transmit energy to distant locations. An example of this can be seen in Figure 1.

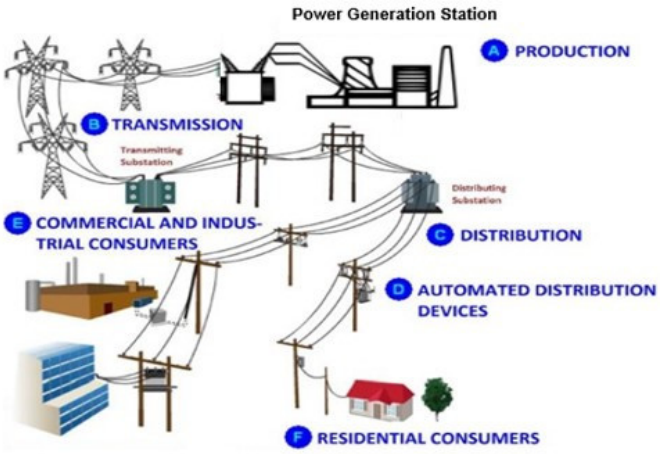

Figure 1: Centralized distribution representation [6]

The second one, the decentralized way, is constituted mainly by microgrids, small scale electricity systems that can work independently to the main electricity grid and are composed of several small power generators, converters and loads close to each other [7]. One representation of a Microgrid can be seen in Figure 2, which shows a non-isolated microgrid, that uses solar energy and other RES, as well as a backup generator and battery storage to feed a set of users, without complex transmission grids.

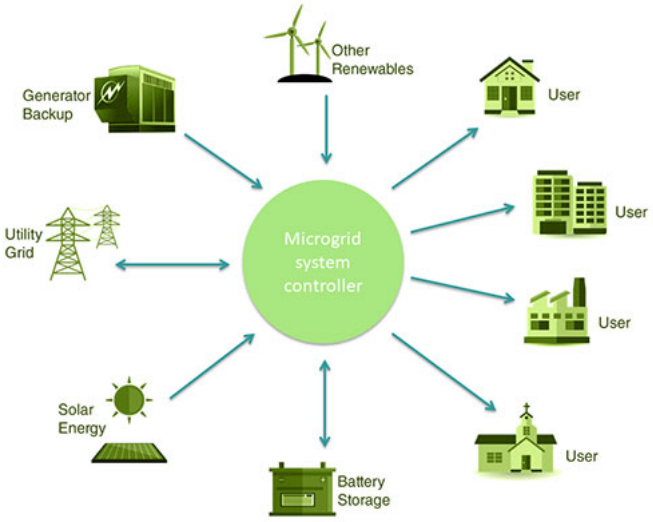

Figure 2: Microgrid representation [8]

In Chapter 1, the advantages and drawbacks of both approaches will be extensively discussed, as well as the choice between choosing DC or AC microgrids. As we will see, there is a strong case in favour of DC Microgrids, due to the rapidly drop in RES's levelized cost of energy (LCOE), which makes microgrids economically viable, and the growing share of DC loads in today's society, result of an increase in the semiconductor devices' usage. For these reasons, this thesis will focus on DC Microgrids.

Having decided for that, it is essential to understand the importance of adapting voltage levels at different points of the grid, a need that comes from different voltage levels of generation units, loads and batteries, dependent on the manufacturer constraints.

In order to correctly meet these constraints, we should use power converters, electronic devices that employ switched-mode circuitry to change DC voltages and currents with efficiencies approaching 100% [9]. In order to chose the best power converter to use in our microgrid, we need to consider some variables, such as their efficiency, if they can be used to step-up or down the voltage level, their price and others. The wide range of power converter's types, their different principles of operation and their different control approaches makes their correct choice essential in developing microgrids and, for that reason, they will be extensively discussed in this study.

In this thesis DC-DC power converters are studied under the context of implementing RES in DC microgrids. Our main objective is to model a real microgrid, select the best DC-DC converters to use in it, define a clear and practical way of controlling these converters and analyze the effects of different loads working in parallel on each other.

This thesis is divided into the following chapters:

- Chapter 1 discusses the advantages of DC microgrids when compared to other grid approaches
- Chapter 2 discusses theoretical principles and provides simulation results of non-isolated DC-DC converters.
- Chapter 3 discusses theoretical principles and provides simulation results of isolated DC-DC converters.
- Chapter 4 introduces an approach of controlling DC-DC converters.

- Chapter 5 describes the model of the DC microgrid used for simulations.
- Chapter 6 is a discussion of its results
- Chapter 7 is the conclusion of the thesis and key takeaways from it

Chapter 1

DC Microgrids

A microgrid can be defined as a group of interconnected loads and distributed energy resources within clearly defined electrical boundaries that acts as a single controllable entity with respect to the grid, having the possibility of being connected or not to the main grid (grid-connected or island-mode) [10]. They are constituted, mainly, by generation units (GU), energy storage systems (ESS), small scale transmission grids and loads. A generic micro-grid representation can be seeing in Figure 1.1.

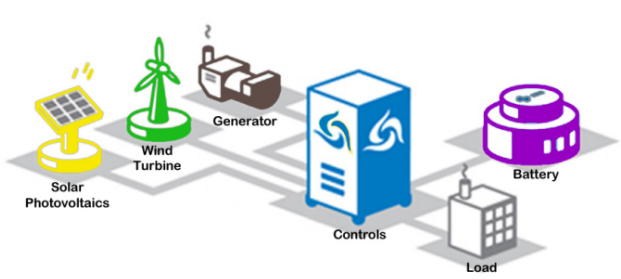

Figure 1.1: Generic microgrid representation [11]

This representation, although very simple, shows us some very important characteristics of microgrids:

- Importance of having more than one generation unit (redundancy): increase grid's reliability as they work in a complementary way.
- Importance of storage systems (battery): as RES usually have fluctuating power production, power demand can be bigger than power offer at some times and smaller at others. Having a storage system is key to accumulate energy and release energy depending on that relation.

- Importance of having a central control system: creates at one specific point in the microgrid, usually the point of common coupling (PCC), where generation units, battery and loads are connected, a voltage reference, stable no matter the conditions.

It is important to notice, as well, that there is not only one type of microgrid available. They can be classified as grid-connected or islanded, when they work without any connection with the main grid, and as AC, DC or hybrid microgrids, depending on the voltage type adopted. A choice between these types needs to be done before advancing into their implementation. In Section 1.1, we will discuss advantages and disadvantages of microgrids, compared to centralized production and will, at the end, argue in favour of islanded microgrids. In Section 1.2, we will argue in favour of DC over AC, mentioning benefits of both choices.

1.1 Microgrids vs. centralized generation

Although a very technologically interesting approach, microgrids are not a rule in today's energy systems, but an exception. This reality originates in the fact that, for decades, most countries promoted centralized generation, through incentives of big nuclear or fossil fuel plants. As a result, distributed generation is limited, even in developed countries, as we can see in Figure 1.2, where only Denmark, that invested for years in RES and cogeneration [12], surpasses 20 % of total electricity production coming from distributed generation.

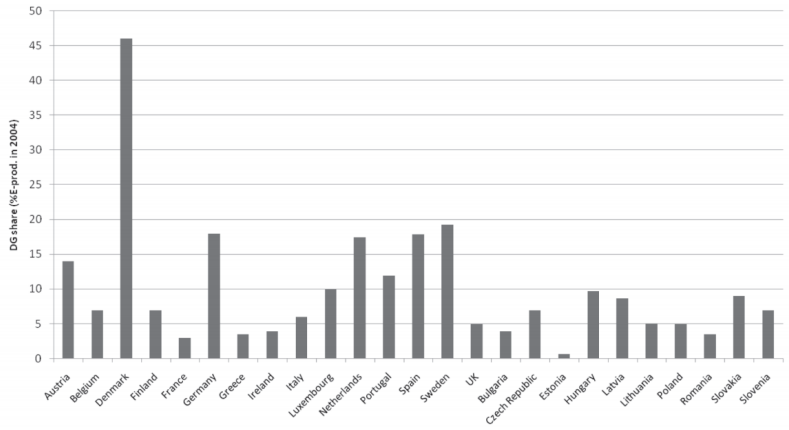

Figure 1.2: Distributed generation shares in total electricity production in 25 EU countries [13]

But why would countries promote centralized generation over microgrids?

This can be easily answered by the fact that, historically, centralized production showed some advantages, specially cost related, when compared to decentralized production. An extensive comparison between both approaches was conducted in [12] and its key conclusions are mentioned below.

1. **Advantages of centralized production**
   (a) Economies of scale: having bigger generation units makes it possible to decrease marginal cost of electricity.
   (b) Reliability: historically, it was easier to spread the energy reliance on several big generation units, connected through complex transmission grids, as they presented bigger efficiencies and smaller costs. Microgrids were, in the past, usually dependent on a specific generation source, such as PV or fuel cells.
2. **Drawbacks of centralized production**
   (a) Transmission losses: as transmission networks gets larger, line losses increases as well, resulting on bigger transmission and distribution (T&D) costs (more than 5% of the energy generated in the United States are lost in T&D).
   (b) High maintenance investments.
   (c) Environmental impacts: centralized generation are highly reliant on fossil fuels and nuclear sources.
3. **Advantages of microgrid production**
   (a) Generation units' cost reduction: because of technological enhancements, microgrid implementation costs shrunk considerably.
   (b) Transmission losses: smaller due to reduced line lengths.
   (c) Environmental impact: allow the easy implementation of RES.
4. **Drawbacks of microgrid production**
   (a) Reliability risk: it is very easy to use DG only based on one energy source, like wind energy, because that would be better suited for a specific region. This can cause problems when facing sudden condition changes, which can cause shortage of production, leading to supply problems.

(b) Architecture of electricity sector: current infrastructure was not originally built to accommodate large proportion of distributed generation.

From the list presented above, it is clear that the historical choice in favour of centralized production was mainly based on cost concerns. In that approach, even if we had more transmission losses due to bigger transmission lines, the economy of scale from big centralized generation units guaranteed smaller final cost of energy. It is also clear, from the points mentioned above, that the environmental impact was not taken into account when making the decision for centralized generation and, nowadays, it needs to be considered.

Regarding the cost, in fact, a couple of decades ago having big non-renewable plants was cheaper, but this situation has changed. Nowadays, as RES's technology evolved, their cost dropped rapidly, as we can see in Figure 1.3. There, it is clear that, in the last 10 years, the levelized cost of energy (LCOE) of solar PV - crystalline has dropped 89% and wind's has dropped 70%, which makes them even cheaper than coal and nuclear generation.

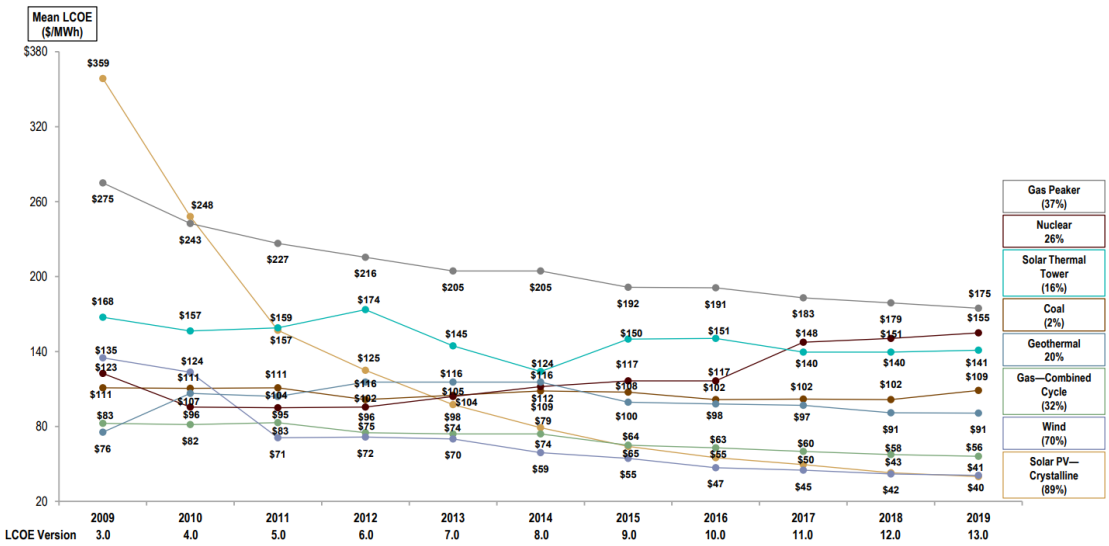

Figure 1.3: Selected Historical Mean Unsubsidized LCOE Values [14]

This would be, by itself, a major argument in favour of microgrids, but it does not stop there. As we have, today, several cost competitive RES in the market, such as PV, wind, fuel cells and others, the reliability risk is severely reduced, as we can easily develop redundant microgrids, which would not rely only on one source to provide energy.

The other drawback of microgrids mentioned was the fact that the today's electricity sector's architecture does not accommodate a large proportion of distributed generation. This would in fact be a problem, but, as we mentioned, one type of microgrid available is the isolated one, where the microgrid is not connected to the main grid, as it is reliable enough to guarantee, on its own, the power needed to all loads connected to it.

Because of the facts mentioned, this thesis will focus on microgrids that are based on renewable energy, redundant to increase reliability and isolated, as an alternative to centralized and fossil fuel or nuclear fed grids.

1.2 DC vs. AC Microgrids

As we saw in the previous section, technological improvements may change electrical paradigms, as it did with respect to the dichotomy of centralized and distributed generation. The same can be seeing in the current flow type of our power systems, that is, the choice between alternated current (AC) and direct current (DC). Discussions regarding this topic dates back to the late 19^{th} century, during what was called the "War of Currents", when the two options were presented by Nikola Tesla and Thomas Edison, respectively.

Ultimately, Tesla's idea prevailed when Westinghouse Electric Company showed that AC distribution guaranteed cheaper prices when compared to Edison's DC one. Back then, this happened mainly because, as centralized power generation was significantly cheaper than distributed generation, for reasons mentioned in Section 1.1, it was necessary to reduce, as much as possible, transmission losses, as distances were higher, a duty the the AC model did better than the DC one. Other than that, back then AC loads were very significant, as most street lighting was using this technology, and they represented a considerable share of all loads [11].

Although these premises were true for almost a whole century, the choice for Tesla's AC systems was unable to take into account some technological advancements made since. Not only the paradigm of centralized vs distributed generation changed (and therefore the crucial necessity of reducing transmissions losses), but the introduction of semiconductors was made. These devices, that are the support to all transistor technology and, thus, all electronics that are based on it, depend on DC power to function. Today, the usage of semiconductors is so disseminated that it is estimated that nearly 80% of all electricity passes through semiconductor components [15], a share that is estimated to increase for the next years.

Having understood this, it is central, in order to chose between AC and DC microgrids, to evaluate the impact that the conversion from AC to DC or vice-versa would have in the system's energy efficiency. If we designed an AC microgrid, we would have, essentially, to make two conversions: between the RES and the transmission system and between the transmission system and the loads. The first one would happen because the majority of RES produce DC power, such as PV and fuel cells [15], and we would need to convert this DC voltage into AC to make the transmission to the loads. The second was due to the fact that, as we have a growing share of DC loads, due to the importance of semiconductor devices, we would need to make a conversion to feed the loads from the AC transmission system. It is estimated that systems where these two conversions are required present conversion losses that are very significant, affecting the efficiency of the global system in up to 20% with only these conversions [11].

Based on this, in [16], a comparison was made between an AC and a DC microgrid, powered only by PV panels and varying the DC load ratio of the grid. As expected, as the percentage of DC loads increased, the DC microgrid losses reduced and the AC microgrid losses increased. The turning point was when the system presented around 30% of DC loads, a point from which the DC microgrid showed a better efficiency, as we can see in Figure 1.4.

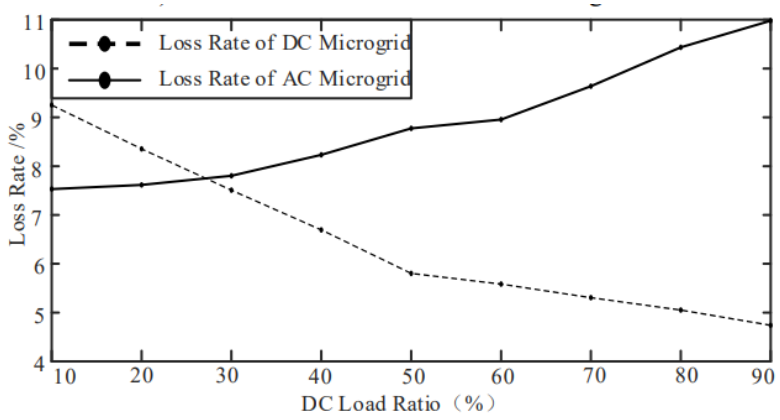

Figure 1.4: Variation curve of loss rate of AC and DC distributed system [16]

As the turning points presents itself with rather low DC loads' ratio, we can conclude that, had the war of currents happened today, Edison's alternative would possibly succeed over Tesla's. For this reason, this thesis will focus its attention on DC microgrids.

Having decided to focus our attention on DC microgrids, we need to understand that one of the main characteristics of a DC system is the need to adapt its voltage levels, as loads require different ones and sources do not produce steady ones. This adaptation is made through power electronic devices, called DC-DC converters. They can be divided into two main categories, the non-isolated DC-DC converters and the isolated DC-DC converters, which will be our focus on chapters 2 and 3.

Chapter 2

Non-isolated DC-DC converters

DC-DC converters are high-frequency electromechanical devices that that take a source of direct current (DC) and, through a correct association of transistors, inductors, capacitors and other elements, convert it from one voltage level to another. Their importance rely on the fact that generation units and loads have different voltage level requirements, what calls for these conversions, even if they both work on DC mode.

Based on this definition, we can clearly understand that we will have two applications for these converters: we could either need a converter to step-up (increase) a voltage level or to step it down (decrease). Based on that, three simple converters were initially developed and they will be the focus of this chapter. They are:

- Buck Converter: step down the voltage level
- Boost Converter: step up the voltage level
- Buck-Boost Converter: step up or down the voltage level

All three converter types rely on a transistor, usually MOSFET or IGBT, and a diode to alter the voltage level. Their principle of operation, as it will be discussed in the following sections, is based on the status of this transistor (ON or OFF), which will make the current to flow in two different ways and, therefore, to regulate the output voltage level. That being said, one important variable that we will take into account when analyzing these converters is the transistor's duty-cycle (θ), that is, the amount of time that it is closed in a given period of time.

2.1 Buck Converter

As mentioned, the Buck Converter is used to step down the voltage level of a DC source and it does that through the correct association of a transistor and a diode. The idea here is to reduce the voltage by stepping up the current, trying to maintain, as much as possible, the energy conserved. In Figure 2.1, we can see the complete circuit of the converter.

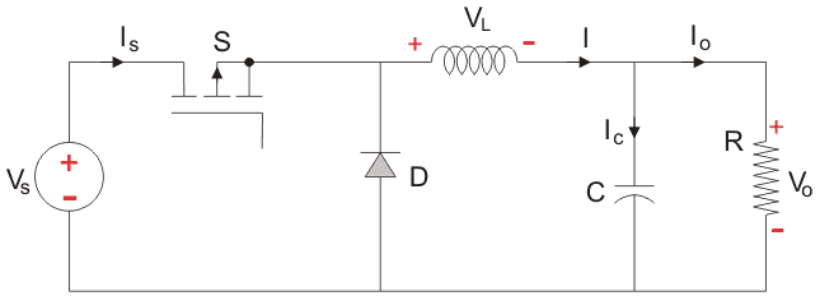

Figure 2.1: Buck Converter Circuit [17]

2.1.1 Principle of operation

The operation of the Buck Converter can be to be divided in two different moments: when the switch is turned ON (closed) and when it is OFF (opened).

Switch is ON (θ): When the switch is closed, current flows directly from the voltage source (V_s) into the inductor, making its magnetic field to increase, storing energy. This will polarize the inductor in the way showed in Figure 2.1. The diode, at this moment, is blocking the current from flowing through its terminals.

Switch is OFF ($1 - \theta$): When the switch is open, current from the voltage source can not reach the inductor, so it will be the inductor, through the energy stored when the switch was closed, that will feed the circuit composed of itself, capacitor, load and diode. It is in this moment, then, that the inductor is acting as a current source, with polarity opposed to the one presented on Figure 2.1 and the diode is providing a path for the current to flow in the circuit, closing it.

As we can see from these two moments, the inductor assumes a very important job of being the component that will make the transfer of power, storing it when the switch is ON and releasing it when it is OFF. This behaviour can be easily seen when we analyze the inductor's current, that increases when the switch is ON

(energy being stored) and decreases when it is OFF (energy being released), as it is showed in Figure 2.2, done through MATLAB/ Simulink simulations.

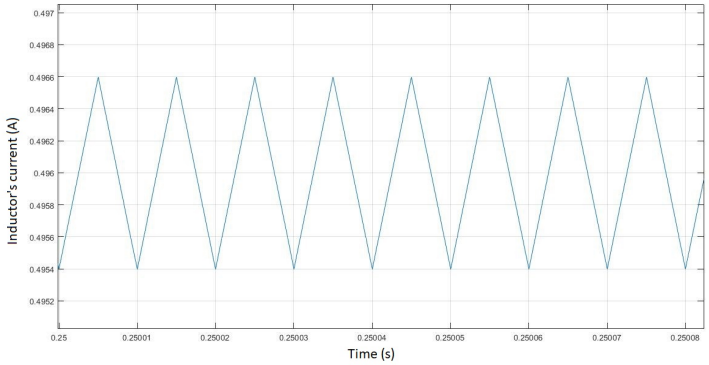

Figure 2.2: Steady-state current in inductor - Buck Converter

As the name of the figure suggests, at this moment we are in steady-state, which means that the value of the inductor's current needs to be the same at the beginning and end of a given period, that is, the energy received by the inductor when the switch is turned ON should be the same as the one provided by the inductor when the switch is turned OFF. It is based on this behaviour that we can find the relation between the input and output voltages of the Buck Converter, developed in the equation below:

$$\begin{aligned} slope_{ON}.time_{ON} &= -slope_{OFF}.time_{OFF} \\ slope_{ON}.\theta.T &= -slope_{OFF}.(1-\theta).T \\ \frac{V_L^{ON}}{L}.\theta.T &= -\frac{V_L^{OFF}}{L}.(1-\theta).T \\ \frac{(V_s - V_{out})}{L}.\theta &= -\frac{-Vout}{L}.(1-\theta) \\ \theta.V_s - \theta.V_{out} &= V_{out} - \theta.V_{out} \\ V_{out} &= \theta.V_s \end{aligned} \tag{2.1}$$

This equation is crucial in the Buck Converter's understanding. As we can see, the relation between the input and output voltage is only dependent on the duty-cycle (θ) of its transistor and, as it can assume values from 0 to 1, we can confirm that the converter can only be used to step-down the voltage level.

2.1.2 Design of Converter

As we can imagine, in order for a converter to work properly, there are some conditions that we need to guarantee on its design when selecting its components. As we can see from Figure 2.1, the main components that we need to set are its inductor and its capacitor.

For the inductor, as discussed above, its main contribution for the converter's proper work is the storing of energy when the transistor is closed and the releasing of it when it is opened, a behavior that was made clear in Figure 2.2. Due to this, we can say that we will have a minimum possible value for its inductance, as, if was is too small, it would not be able to store and provide enough energy for the load.

In practical terms, as we increase its inductance, the peak-to-peak amplitude of its current, shown in Figure 2.2, decreases. If we had an inductance that was too small, the value of the current could decrease a lot and reach zero, when, at this moment, the diode would prevent the current from flowing in the opposite direction (current will never be negative). This means, in terms of design, that the peak-to-peak amplitude of the inductor's current cannot be bigger than twice its average, otherwise the correct functioning of the converter is not guaranteed. Figure 2.3 shows a situation where the design was not made properly, with the inductance not big enough, and therefore we have a moment where the diode is blocking the current.

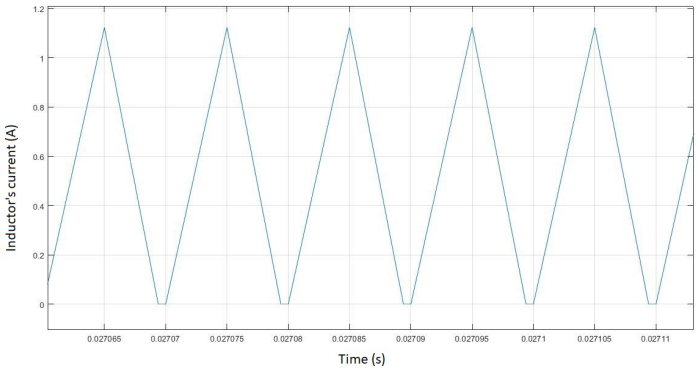

Figure 2.3: Current in the inductor in discontinuous mode

When this happens, we are in what is called the discontinuous mode, and the relation given by equation 2.1 is no longer true, as the inductor is not able to store enough energy when it is being charged. It is very interesting to investigate what happens when we reach this mode. From an intuitive point of view, we can think

that, if its inductance was zero, the inductor would behave as a short circuit and, therefore, the output voltage would tend to the input one, assuming that we have a capacitor big enough to reduce its ripple. This behaviour can be seen in the figure below, where we show the normalized voltage, that is, a relation between input and output voltage ($\frac{V_s}{V_{out}}$) compared to the normalized current in the inductor, for several values of duty-cycle (in here represented by D).

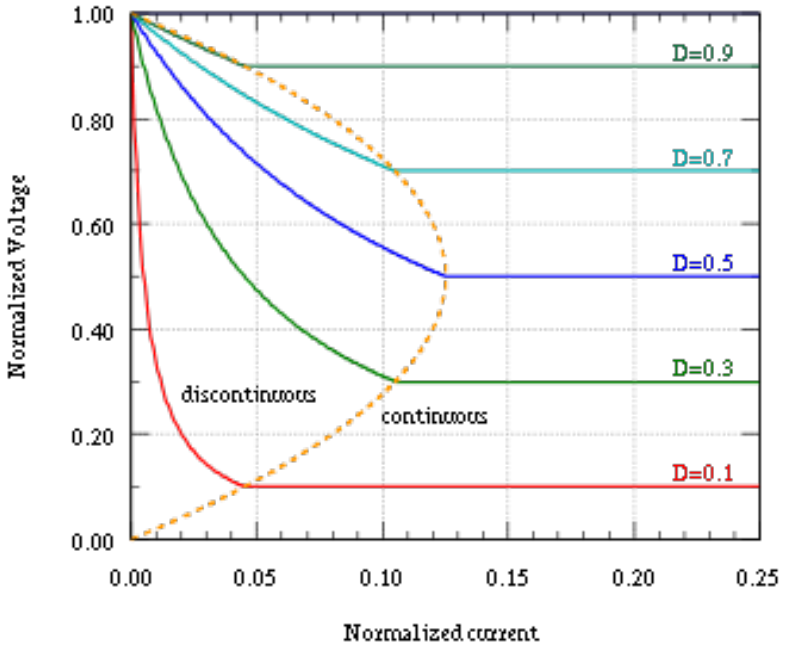

Figure 2.4: Output voltage in discontinuous mode - Buck Converter [18]

It is clear that, as we reduce the normalized current (reduce the value of the inductance), we reach the discontinuous mode zone, where the relation 2.1 is no longer true. As we continue to reduce it, the relation between input and output current tends to one, therefore the effect of the Buck Converter is being bypassed.

As it was mentioned before, in order to avoid the discontinuous mode, we need to ensure that the average value of the inductor's current is bigger than half the amplitude of that current. Based on this, it is important to calculate the minimum inductance value that would guarantee that the system is working in continuous mode, which is done as follows:

$$
\begin{aligned}
\frac{\Delta I_L}{2} &\leq I_{L,avg} = I_{o,avg} \\
\frac{\Delta I_L}{2} &\leq \frac{V_o}{R} \\
\frac{\Delta I_L}{2} &\leq \frac{\theta.V_s}{R} \\
\frac{I_{L,\theta T} - I_{L,0}}{2} &\leq \frac{\theta.V_s}{R} \\
\frac{I_{L,0} + \frac{V_s.\theta.T(1-\theta)}{L} - I_{L,0}}{2} &\leq \frac{\theta.V_s}{R} \\
\frac{V_s.\theta.T(1-\theta)}{2.L} &\leq \frac{\theta.V_s}{R} \\
L &\geq \frac{R.T.(1-\theta)}{2}
\end{aligned}
\tag{2.2}
$$

The other component that is important for the design of the Buck Converter is the output capacitor seen in Figure 2.1. Its function is to reduce the voltage ripple in the load, caused by the current ripple in the inductor. The minimum value of this capacitor is given, as it was extensively discussed in [19], by the following equation.

$$
C_{out} = \frac{\Delta I_L}{8.V_{out,ripple}.F_{sw}} \tag{2.3}
$$

2.2 Boost Converter

The second type of DC-DC converters that we will study in this thesis is the Boost Converter and, as it is clear from its name, it is used to step-up the voltage level of a given voltage source. As we can in the figure below, this converter has a structure that is similar to the one of the Buck Converter (Figure 2.1), that is, it is composed by an inductor, a capacitor, a diode and a transistor.

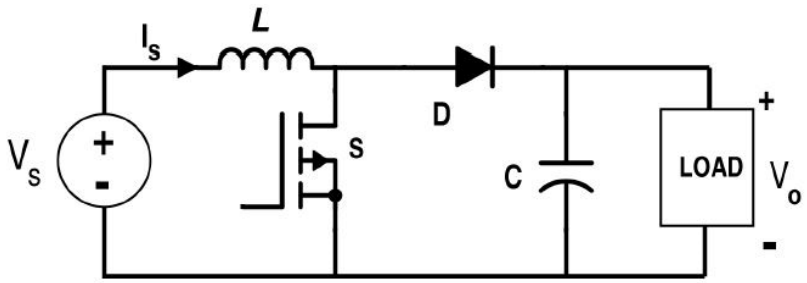

Figure 2.5: Boost Converter Circuit [20]

2.2.1 Principle of operation

Also in here, the association between the transistor and the inductor is key in the stepping up of the voltage, as is the diode, providing a path to the current at some moments and blocking it at others, as we will discuss in more details below. Again, the operation of this converter is going to be divided in two moments, when the transistor is closed and when it is opened.

Switch is ON (θ): When the transistor is closed, we have a closed circuit containing the voltage source (V_s) and the inductor (L), what makes the current that flows through the inductor to be very high. This will lead the inductor to store a lot of energy due to the variation of its magnetic field, i.e. the inductor gets charged. At this moment, the load is being fed only by the capacitor and the diode is isolating both circuits.

Switch is OFF ($1 - \theta$): When the transistor is opened, the current flowing through the inductor is significantly smaller, compared to when it was closed, due to the addition of the capacitor and load to the circuit involving the source and the inductor. This drop in the current will make the inductor's magnetic field to collapse, releasing the energy that was stored in it, which will make the voltage in the load to increase, as it will see an addition of effect of the voltage source and the inductor, i.e. voltage source and inductor source are seen as in series at this moment.

As we can see, the current seen in the inductor here is, as well, key in the transfer of power from source to load. Again, this current will have a triangular shape, representing the inductor being charged when the transistor is closed and discharged when it is opened, as we can see in figure 2.6.

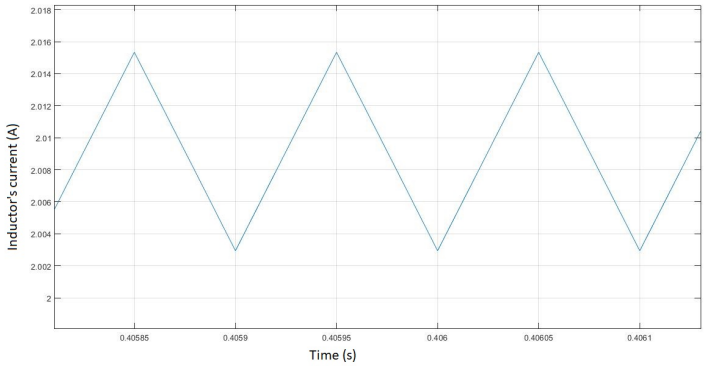

Figure 2.6: Steady-state current in inductor - Boost Converter

The relation between the input and output voltages can be found by analyzing this current in steady-state, as its variation in one period needs to be zero. We also know that, when the switch is ON, the voltage across the inductor has the same value as voltage source (V_s) and, when the switch is OFF, it is the difference between the input and output voltages ($V_s - V_o$). Based on that, we can find the Boost Converter's voltage relation as follows:

$$\begin{aligned} slope_{ON}.\theta.T &= -slope_{OFF}.(1-\theta).T \\ \frac{V_s}{L}.\theta.T &= -\frac{V_s - V_o}{L}.(1-\theta).T \\ V_s.\theta &= (V_o - V_s).(1-\theta) \\ V_s.\theta &= V_o - V_o.\theta - V_s + V_s.\theta \\ V_o &= \frac{1}{1-\theta}.V_s \end{aligned} \tag{2.4}$$

As the duty-cycle can assume values from zero to one, the Boost Converter can only increase the output voltage, as shown in the above equation.

2.3 Buck-Boost Converter

In the previous two sections, we discussed two converters that could step-up or step-down the voltage level of a given voltage source. In this section, we will talk about a converter that can do both, called Buck-Boost Converter. We can see its circuit in the following figure.

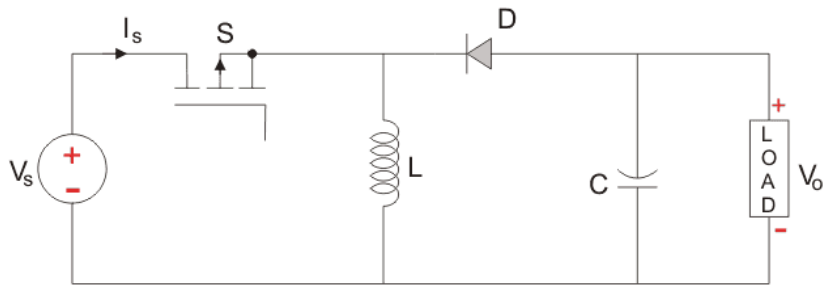

Figure 2.7: Buck-Boost Converter Circuit [21]

As we can see from this figure, the resemblance with the two precious converters is clear, as it is composed of a transistor, diode, inductor and capacitor, as well as the voltage source and the load.

2.3.1 Principle of operation

As we saw in the previous two converters, the operation of the Buck-Boost Converter can be divided in two moments, when the transistor is closed and when it is opened.

Switch is ON (θ): As well as for the Boost Converter, in here, when the transistor is closed, current is flowing only in the inductor, what would lead to an increase in its magnetic field and, consequently, the charging of it. Also, in this stage, the diode is reverse biased, so it will block the current from flowing in the direction of the load, which means that the load is fed only by the capacitor.

Switch is OFF ($1 - \theta$): When the transistor is opened, the voltage source is disconnected from the rest of the circuit, which leads the inductor to start discharging, providing energy to other components. At this moment, the diode is providing a path for the current, connecting the load and capacitor to the inductor. Giving the direction of the current, the voltage in the load, at this moment, would assume negative values, when using the convention of the Figure 2.7.

As we saw in both the Buck and Boost cases, the main device in here is the inductor, as it is being charged and discharged depending on the transistor status. Also in here, the shape of the current's curve will be triangular, as we can see in Figure 2.8.

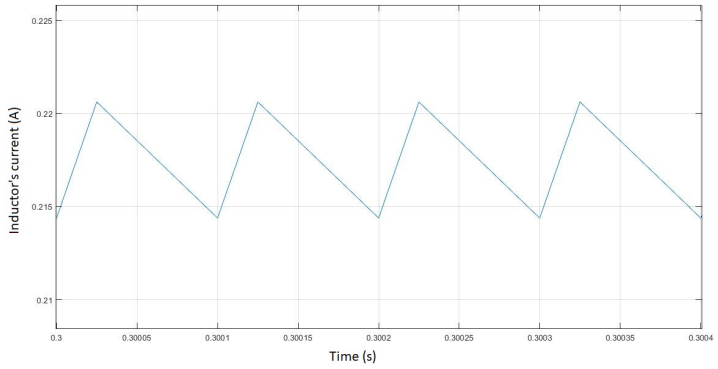

Figure 2.8: Steady-state current in inductor - Buck-Boost Converter

It is also from this figure that we will be able to get the relation between its input and output voltages, as we know that, in steady-state, the ascending time's slope times its period should be equal to the descending time's slope times its period. We also know that, when the transistor is closed, the voltage across the inductor is the source's voltage (V_s) and when the transistor is opened is the negative of the load's voltage ($-V_{out}$), as the diode is conducting. Based on this we can find its relation as follows.

$$\begin{aligned} slope_{ON}.\theta &= -slope_{OFF}.(1-\theta) \\ \frac{V_s}{L}.\theta &= -\frac{-V_o}{L}.(1-\theta) \\ V_s.\theta &= V_o - V_o.\theta \\ V_o &= V_s\frac{\theta}{(1-\theta)} \end{aligned} \tag{2.5}$$

It is interesting to note that, as the duty-cycle can assume values from zero to one, this converter can, based on the above relation, either step up or down the input voltage.

2.4 Non-isolated converters' Comparison

As we discussed above, the main difference between the three types of non-isolated converter is the use that they have. The Buck Converter can only be used to step-down a voltage level, as the Boost Converter can only be used to step-up the voltage level and the Buck-Boost Converter can be used to do either. The following figure shows a comparison of the input-output relations presented in questions 2.1, 2.4 and 2.5, when varying the duty-cycle value from zero to one.

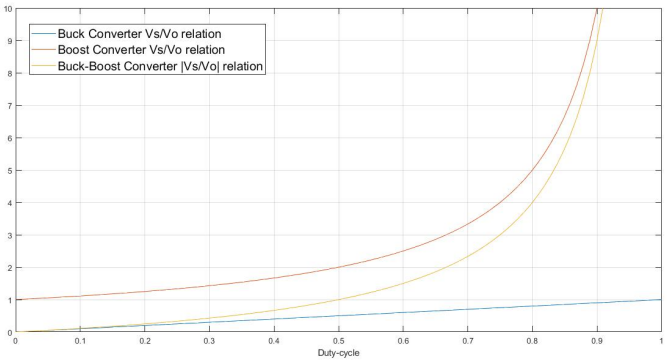

Figure 2.9: Output-input relations of the three converters

It is important, as well, when comparing different types of converters, to evaluate their energy efficiencies. As we mentioned in the beginning of this chapter, these converters aim at changing the voltage level, by varying the current in the load, trying to keep a 100% energy efficiency. As we can imagine, maintaining it at 100% is not possible, as we have some losses in the process, due to transistors, internal resistances and others.

In order to check their real efficiencies, all three types were modelled on MATLAB/ Simulink and their efficiencies are showed in Table 2.1, as well as the parameters for each of the models used 2.2.

Table 2.1: Non-isolated converters' efficiencies

Type	**Efficiency**
Buck Converter	98%
Boost Converter	98%
Buck-Boost Converter	93%

Table 2.2: Parameters used to calculate non-isolated converters' efficiencies

Converter type	**Parameter**	**Value**
ALL	Transistor internal resistance	1mΩ
	Transistor forward voltage	1mV
	Switching frequency	10kHz
	Duty-cycle	0.5
	Diode internal resistance	1mΩ
	Diode forward voltage	0.8V
	Input voltage	100V
Buck	Capacitance	100μF
	Inductance	210mH
	Load resistance	100 Ω
Boost	Capacitance	5μF
	Inductance	125μH
	Load resistance	100 Ω
Buck-boost	Capacitance	500μF
	Inductance	24μH
	Load resistance	100 Ω

It is important to mention that the efficiencies of Table 2.1 are aligned with the literature regarding non-isolated converters, as we can see in [22] and [23]. The main reason for the efficiencies found to be little superior to the ones of the two references is the fact that, in our model, not all losses were considered, as for example the losses in parasitic resistances in inductors and capacitors.

Chapter 3

Isolated converters

The main difference between isolated and non-isolated converters is the fact that first ones detach their inputs from their outputs by electrically and physically separating them, usually through the use of transformers [24]. This prevents current from flowing directly from one side to another, although energy is still transferred through transformers' electromagnetic fields.

By using them, we can have some benefits, as mentioned below:

- Safety compliance: specially from converters connected to high and hazardous voltages, isolation separates the output from dangerous input voltages [24].
- Breaking ground loops: because primary and secondary sides do not share a ground, isolation can be interesting to break ground loops, specially in circuits that are sensitive to noise [24].
- Another degree of freedom in the input-output voltage relation, given by the number of turn ratio (n) of the transformer.

Specially because of the safety advantage, isolated converters are needed in some applications, such as for medical devices [25]. Although this is very important, there are, as well, some drawbacks of using isolated converters, with the main ones mentioned below:

- Isolated converters tend to be more expensive because transformers are used instead of simple inductors. The higher the isolation required, the greater the cost [26].
- They are usually larger than their non-isolated versions.

- Their efficiency tend to be much smaller compared to non-isolated converters, as the transformer is a major source of losses in their circuit [26].

As we did for non-isolated converters, we will now mention the main types of isolated converters, describing their principle of operation and providing their circuits. At the end, a comparison between them and the ones presented in Chapter 2 will be done in order to decide which ones we will focus our attention on.

3.1 Full-bridge Converter

The first converter that we need to discuss is the Full-bridge Converter, an isolated DC-DC converter that can be used either to step-up the voltage level or step it down. The figure below show its circuit and the main information that we can get from it is the fact that it is separated by a transformer in primary and secondary sides.

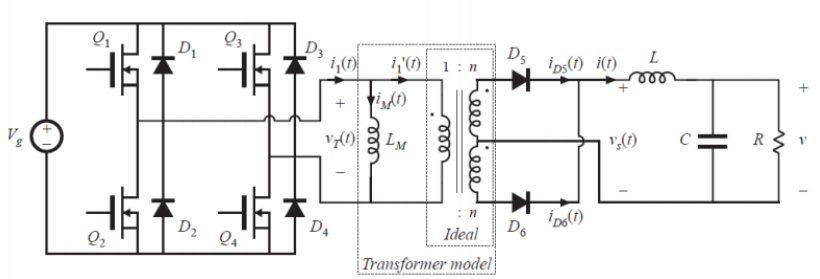

Figure 3.1: Full-Bridge Converter circuit [18]

On the primary side, we have four switches, in the example MOSFETs, associated with diodes in a way that the voltage seen in the primary side of the transformer (V_T) can be either the positive value of the voltage source (V_g), its negative value ($-V_g$) or zero, depending on the state of the switches (ON or OFF). For example, if the switches Q1 and Q4 were closed and Q2 and Q3 were opened, the transformer's voltage would be the same as the source's (V_g), as if the status of the switches were the opposite, it would be the negative value of the voltage source ($-V_g$).

It is important to notice that switches Q1 and Q2 or Q3 and Q4 can never be turned ON at the same time, because this would lead to a short-circuit in the voltage source.

On the secondary side of the transformer, we have two diodes placed in a way that the voltage on the secondary ($v_s(t)$) is positive even if the input voltage of the

transformer is negative. This voltage will be equal to the module of the voltage in the primary side (V_T) multiplied by the number of turns ratio of the transformer (n), which guarantees, as mentioned in the beginning of this chapter, a new degree of freedom for this converter. After that, we have a low-pass LC filter, used to take the average of the voltage $v_s(t)$ and provide a steady DC voltage to the load.

An example of the main waveforms of this converter is presented below, where we can see that the voltage in the secondary side is always positive or zero, even when the voltage in the primary side assumes negative values (switches Q2 and Q3 conducting).

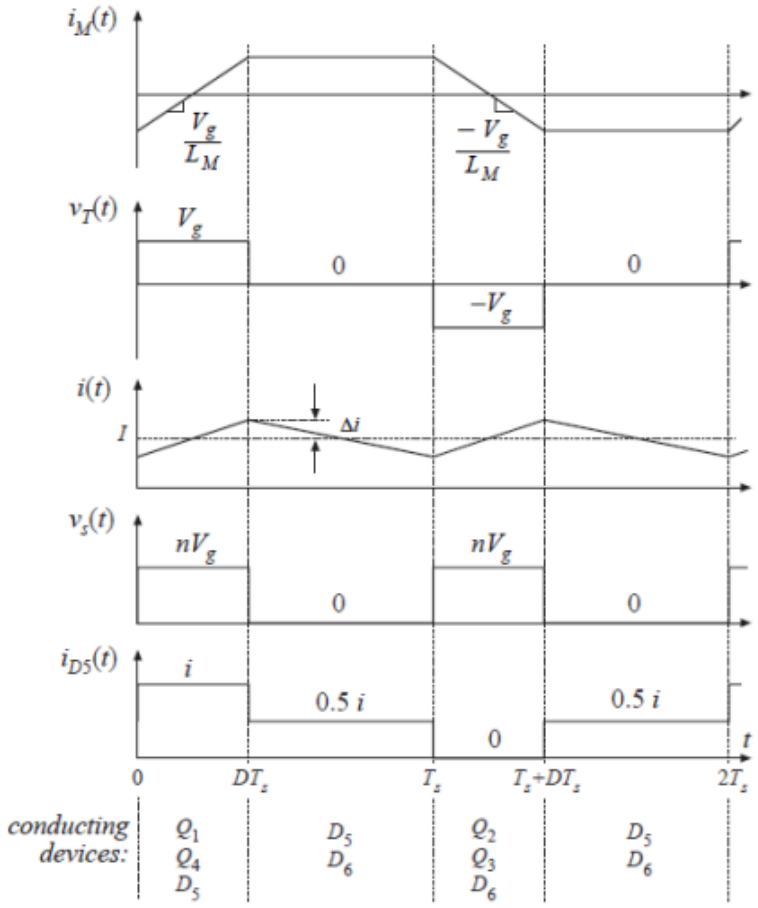

Figure 3.2: Main Full-bridge Converter's waveforms [18]

Based on the described principle of operation, we can understand that the output voltage will be dependent on the duty-cycle of the primary side's switches (θ) and the number of turns ratio of the transformer (n). It important to explain

that the duty-cycle, in here, represents the amount of time in a given period that the transistors Q1 and Q4 are conducting or that the transistors Q2 and Q3 are conducting, that is, the amount of time that the primary side of the transformer has a voltage level different than zero. Finally, the voltage relation of this converter can be seen below:

$$\frac{V_o}{V_g} = n.\theta \tag{3.1}$$

3.2 Half-bridge Converter

Although the principle of operation of the Full-bridge Converter looks interesting, its efficiency, as we will show later in this chapter, is considerably small. As it was already mentioned, transformers are great contributors of this losses, but they are not the only one.

A second considerable contributor of these losses are the transistors, with two types of losses involved on them: conduction and commutation. Conduction losses appear because, even when the transistor is closed, there is a small voltage difference across its terminals and, because there is a current flowing through them, energy is being consumed. For the second type of losses in transistors, the commutation ones, when the transistor is being closes, there is a overlap of a moment where the voltage difference is going down and the current is going up, which lead to power being lost. Both this losses can be seen in the figure below.

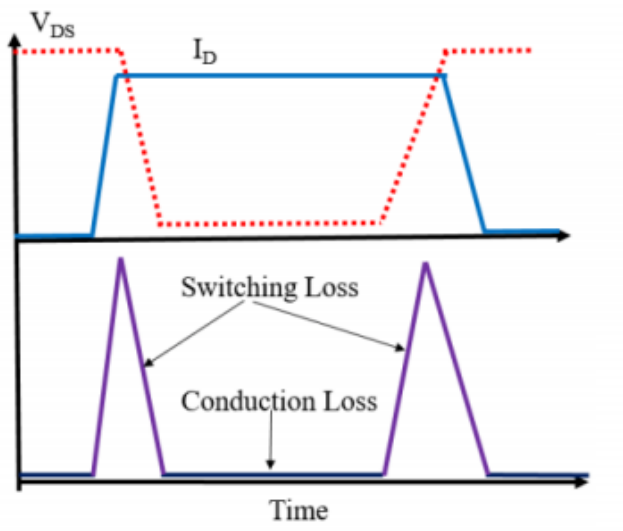

Figure 3.3: Transistor losses: commutation and conduction [18]

Due to that, one improvement that we can do on the Full-bridge Converter is to reduce its number of transistor. One of the ways to do that is by implementing the Half-bridge Converter, where two of the four transistors are substituted by capacitors, as we can see in the figure below.

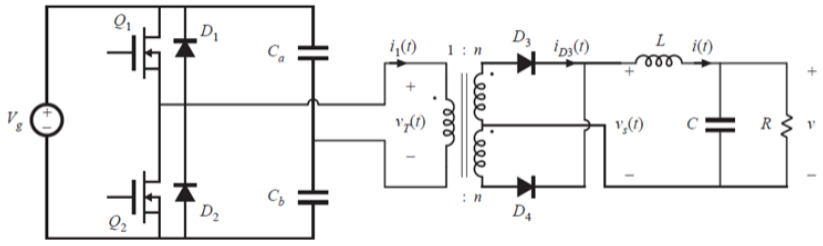

Figure 3.4: Half-Bridge Converter circuit [18]

The resemblance with the Full-bridge is clear, as its secondary side remains the same. As mentioned, the main difference is the substitution of two transistors by capacitors, usually of same magnitude, in a way that the negative connection of the transformer will always have half of the voltage level of the source ($\frac{V_g}{2}$). Because of that, the voltage level V_T will be defined only by the two remaining transistors, in a way that, if Q1 is closed, the voltage at the transformer would be half the voltage level of the source ($\frac{V_g}{2}$) and, if Q2 is closed, its negative value ($-\frac{V_g}{2}$).

As for the secondary side, the principle remains the same. The arrangement of the diodes guarantees that the voltage V_s will always be positive, no matter the input voltage of the transformer and we still have a low-pass LC filter to provide a steady DC level voltage to the load.

This modification does present some efficiency improvements when compared to the last converter, but not without drawbacks. The main drawback is that, with the voltage in the primary side being at most $\frac{V_g}{2}$, the output voltage level is limited, as the output-input relation of this converter is:

$$\frac{V_{out}}{V_g} = \frac{\theta.n}{2} \tag{3.2}$$

3.3 Forward Converter

Another type of isolated converter is the Forward Converter, that can also be used to either step-up or down the voltage level of a given voltage source. As we can see from its circuit, presented in Figure 3.5, it is divided in primary, secondary and tertiary sides by a transformer.

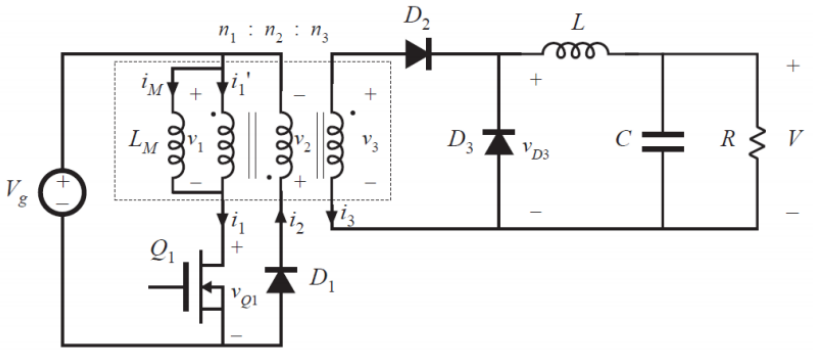

Figure 3.5: Forward Converter circuit [18]

In this converter, on its primary side, we have only one transistor. When it is closed, we have a close circuit made of the voltage source, the primary side of the transformer and the transistor. At this moment, the voltage provided to the primary side of the transformer is reflected to its tertiary side, making diode D2 to conduct. When the transistor is opened, we have two different moments of operation. First, the diode D1 will provide a path for the magnetizing current to flow, avoiding the saturation of the transformer, while, at the same time, the diode D2 is in reverse biased mode (blocking the current to flow through its terminals) and

the diode D3 is conducting. Second, when the magnetizing current is completely dealt with, diode D1 stops conducting and, in this moment, we have only diode D3 operating in direct biased mode.

It is important to understand, from the description above, that the OFF period of the switch needs to be big enough for all the magnetizing current to be eliminated in order to prevent the transformer from saturation. In this converter, power is being transferred to the tertiary only when the switch is turned ON, while, during all the OFF period, the diode D2 is blocking that transfer. This behaviour can be seen in the figure below that shows the main waveforms of this converter.

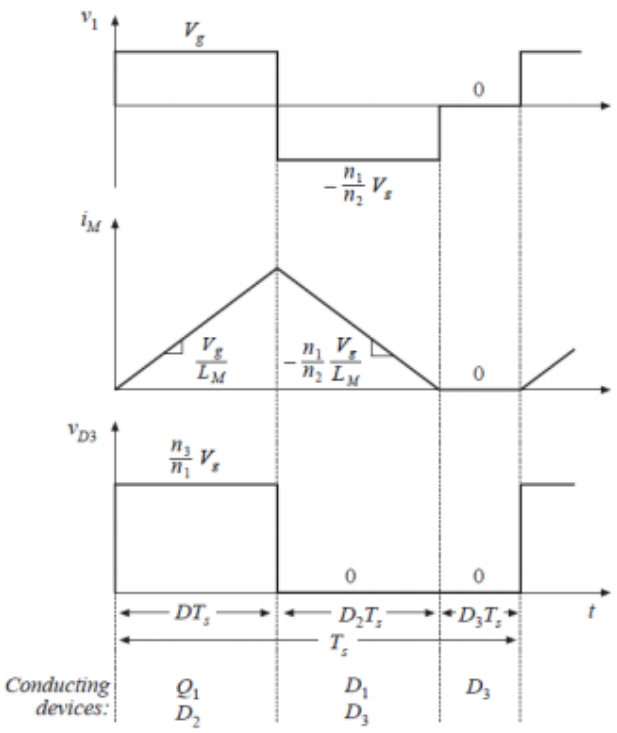

Figure 3.6: Main Forward Converter's waveforms [18]

As we can see, power is being transferred only when the transistor Q1 is conducting, as the voltage across the diode D3 is only different than zero at that moment. Also, the magnetizing current (i_M) is being eliminated when the transistor Q1 is turned OFF, due to the path provided by transistor D1, which makes it important for the OFF time of Q1 to be sufficient enough for the magnetizing current to go to zero, otherwise we would saturate the transformer.

Considering a number of turns ration (n) to be equal to $\frac{n_3}{n_1}$, the relation between the input and output voltage for this converter is:

$$\frac{V_o}{V_g} = n.\theta \tag{3.3}$$

Again, it is clear that this converter can be used to either step up or down the voltage level, depending on the duty-cycle and the number of turns ratio previously defined.

3.4 Flyback Converter

The last isolated converter that we will discuss is the Flyback Converter. Again, this converter can be used to either step-up the voltage level of a given voltage source of step it down. As we can see in the figure below, this converter has a similar configuration as the Buck-Boost one (Figure 2.7), what will be reflected in its output-input voltage ratio.

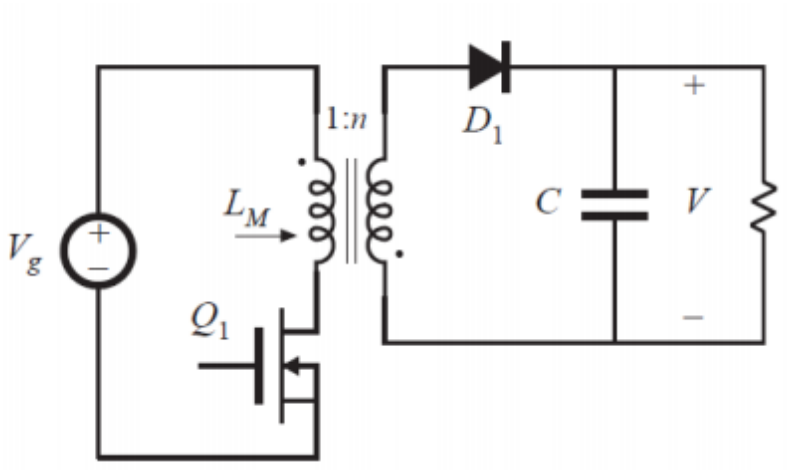

Figure 3.7: Flyback Converter circuit [18]

The operation of the Flyback Converter is a little different from the other isolated converters in a way that, in here, the transfer of power from primary to secondary sides is done when the switch is OFF. When it is ON, the voltage source is charging the magnetizing inductance of the transformer, in here referenced by L_M, and the diode D1 is blocking the current flow in the secondary side. When the switch is finally turned OFF, the magnetizing current is reflected to the secondary

side, with the diode finally conducting, charging the capacitor, which guarantees the voltage level at the load.

The final input-output voltage relation of this converter can be seen below, where it is clear the resemblance with the transfer function of the Buck-Boost Converter (2.5).

$$\frac{V_o}{V_g} = n.\frac{\theta}{1-\theta} \tag{3.4}$$

3.5 Comparison of isolated and non-isolated converters

As we mentioned, the main advantages of isolated converters are the safety that they provide by electrically separating the primary from the secondary side, as well as the fact that all of them have another degree of freedom, the number of turns ratio from the transformers (n). Although these advantages seem interesting, they come with a major setback efficiency related.

As we saw in Table 2.1, the efficiencies of non-isolated converters approached 100%, which is not true for isolated ones, as we can see in the table below.

Table 3.1: Isolated converters' efficiencies

Type	**Efficiency**
Full-bridge Converter	52%
Half-bridge Converter	71%
Forward Converter	88.15%
Flyback Converter	72%

These efficiencies were calculated in [27] and [28] and the simulation was made in the scenario presented in table below:

Table 3.2: Scenario of efficiency calculation on isolated DC-DC converters

Converter type	Half-Bridge Converter	Full-Bridge Converter	Flyback Converter	Forward Converter
Input Voltage (V)	300	300	100	90
Load Voltage (V)	28	28	28	58.03
Power Supply (W)	417	585	385	51.97
Load Power (W)	300	300	300	45.81

Because of the significantly smaller efficiency of these converters, compared to non-isolated ones, they are much less used in real-life applications. Due to this, when implementing our DC Microgrid in this thesis, we will use only non-isolated DC-DC converters, and more specifically Buck and Boost Converters due to their efficiency being significantly higher.

Having chosen the types of converters that we will use in this study, we need to discuss how to control them, that is, how can we provide a voltage reference to a converter and guarantee that its output voltage will be steady at that level? This is the topic of the next chapter, where, not only a control strategy will be defined, but a mathematical approach to set all the control parameters will be shown.

Chapter 4

Control of DC-DC converters

Having decided which DC-DC converters we will use in our study, we need now to focus on how to control them in order to achieve the different voltage levels required by the manufactures of different loads. As we saw in the previous chapters, specifically in equations 2.1 and 2.4, the output voltage of both Buck and Boost converters are defined by the duty-cycle (θ) of their transistors. It is clear, then, that this will be the control variable, with which, given a reference voltage, we will control the output voltage of the converters.

The most common control strategy is the feedback control, using closed loop systems. In these systems, a reference signal is compared to the measured output that we want to control, generating an error signal. This error signal will then be processed by a control unit, which will generate a control signal to be provided to the plant. The plant is a representation of any given process, for example it could a vehicle, that receives as input the amount of fuel going in the motor and provides, as an output, that vehicle's speed. In our models, as mentioned before, the plant would represent the Buck and Boost converters.

The control signal will affect the functioning of the plant in a way to change the measured output, reducing the error. The comparison between the output and the reference value is continuously done in a way to maintain the output steady at the level of the reference. The schematic of this feedback control can be seen in Figure 4.1.

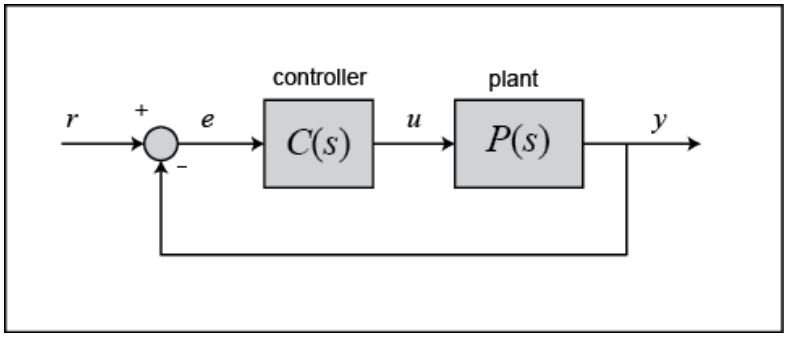

Figure 4.1: Feedback control system schematic [29]

In the case of a voltage converter, the reference signal will be the voltage that we want the output to be fixated at (V_{ref}), the control signal will be the transistor's duty-cycle (θ) and the measured output will be the voltage on the load side (V_{load}). The transistor's state (ON or OFF) is given by pulse width modulation (PWM) signals, from the analog control signal, that is the duty-cycle.

Based on the presented schematic, it is clear that one of the main challenges that we will have when trying to control the output voltage of DC-DC converters will be defining a controller ($C(s)$) that will provide a good response for the whole system. Discussing this controller will be the main focus of this chapter, where we will first discuss a simple, but possible approach for it, on Section 4.1, then discuss an improvement of this approach, on Section 4.2, and finally focus on a mathematical approach to determine the system's parameters that will provide an acceptable output voltage response.

4.1 PID vs PI controller

Having decided for the feedback control system, we need to chose a controller that is more suitable for our application. The most used control unit nowadays is the PID controller, that combines proportional, integral and derivative controllers, with more than 95% of closed loop operations of the industrial sector using it [30].

The first part of this controller is the proportional one, where the control unit multiplies the error signal of Figure 4.1 by a proportional constant (K_p) in order to provide the control signal (θ). The proportional controller is associated to how fast the response to a variation in the reference or the output will be.

The second part of the PID controller, the integral one, is associated to the elimination of the steady-state error. It does that by integrating the error over a

period of time until the error value reaches zero. The integral controller limits the speed of the response to condition changes, but reduces its overshoot.

The last part, the derivative controller, is important to anticipate future behaviour of the error, by giving a kick start for the output and, therefore, increasing system response [30]. In conclusion, P represents the dependency of the present error, I the accumulation of past errors and D is the prediction of future errors [31].

In Figure 4.2, a closed loop control system, similar to the one presented in Figure 4.1, is shown with the controller being PID, with proportional, integral and derivative parameters represented as K_p, K_i and K_d.

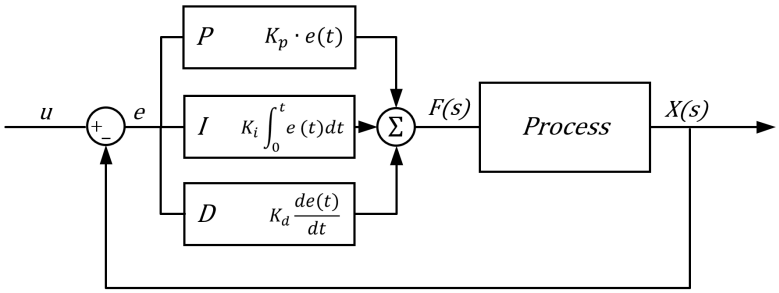

Figure 4.2: Closed loop control with PID control unit [32]

Although the concept of PID controllers is well established in the literature and used in most industrial application, in the context of DC-DC Converters, PI controllers are often favored over PID. This preference was extensively discussed in [33], where a comparison between both control systems was developed in a bi-directional DC-DC converter scenario.

In this document, it was proven that, for both Buck and Boost operation modes of the bi-directional converter, the PI controlled system has a better stability in comparison with the PID one, which meant that the output voltage was less sensitive to variations in the input voltage. In this study, the output voltage was measured for a given input one and, at a certain moment, the input voltage suffered from a perturbation that changed its value. Consequently, the output voltage level changed as well for a brief moment, before coming back to the reference value, and its maximum deviation from the reference was measured, having the PID controlled system showed a bigger one as we can see in the Table 4.1, presented on [33].

Table 4.1: Output voltage response comparison: PI vs PID controller

Operation mode	PI controller		PID controller	
	Input voltage (V)	Output voltage (V)	Input voltage (V)	Output voltage (V)
Boost Operation	45	379	45	102.3
	48	380	48	110
	50	381.5	50	118
Buck Operation	375	47	375	43
	380	47.5	380	44
	385	48	385	46

Another similar and interesting argument in favor of the usage of PI controllers was given by [34], where the authors mentioned that the derivative component of PID controller is associated with significant noise in DC-DC converters. This is mainly due to parasitic resistances and inductances in the output capacitor, shown in Figure 4.3.

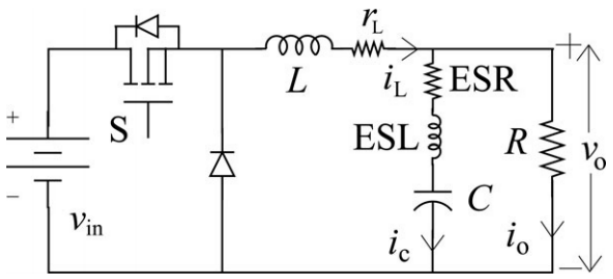

Figure 4.3: Proposed Buck circuit with parasitic resistances and inductances [34]

In order to confirm this behaviour, we did a simulation on MATLAB/ Simulink, for a Buck converter similar to the one presented above. Both a table with the values of all parameters of the Buck converter used and the system's structure are shown below in Table 4.2 and Figure 4.4, respectively.

Table 4.2: Buck converter and control parameters used in noise's simulation

Parameter	**Value**
Inductance (L)	200 mH
Capacitance (C)	100 μF
Load (R)	100 Ω
Parasitic resistance inductor (Rl)	30m Ω
Parasitic resistance capacitor (ESR)	5 m Ω
Parasitic inductance capacitor (ESL)	10 nH
Proportional parameter (K_P)	0.01
Integral parameter (K_I)	0.94
Derivative parameter (K_D)	0.05

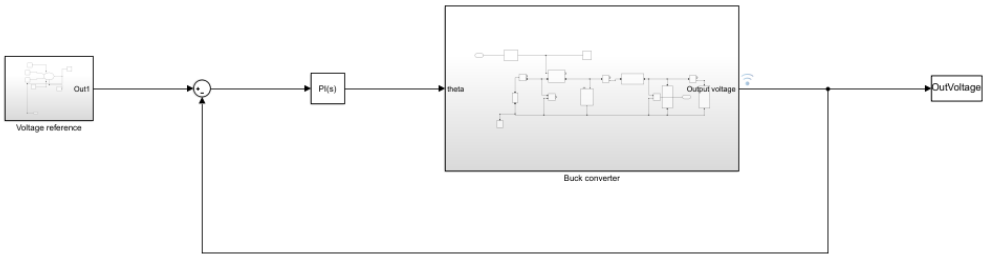

Figure 4.4: Control System - Buck Converter

The results, as expected, confirmed that, in the presence of the derivative controller, the output voltage measured did suffer of an oscillatory nature, even after a considerable amount of time from the beginning of the simulation. This can be seen in figures 4.5 and 4.6, where we show the system's voltage response and a highlight of its oscillation.

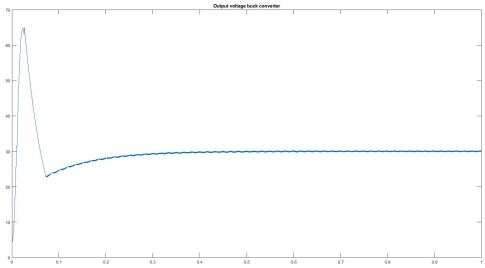

Figure 4.5: Buck Converter's output voltage with PID controller

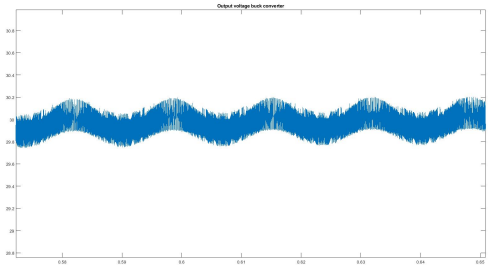

Figure 4.6: Buck Converter's output voltage with PID controller - zoomed

It was important, then, while maintaining the same parameters of Table 4.2, to implement a PI controlled version of the system in order to compare its responses. The results of that simulation are presented in the image below, where it is clear that the oscillatory behaviour of the system was due to the derivative part of the controller, as it is mitigated when we are not using the derivative part of the controller.

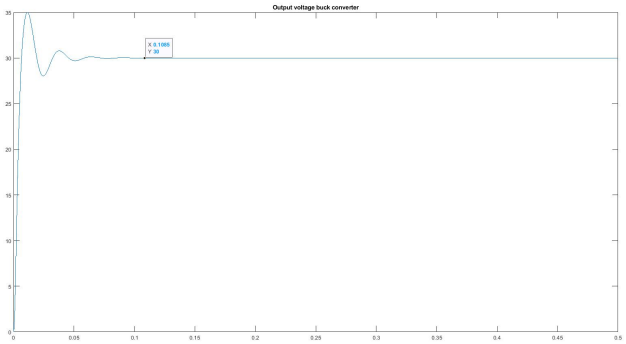

Figure 4.7: Buck Converter's output voltage with PI controller

4.2 Cascade Control

Although a single feedback control system, using PI controllers, seems like an interesting approach, its response to disturbances in the system (on the voltage supply side or the load side) is not as fast as we would like it to be. Because of this, an alternative was proposed on [35], where we would have two PI controllers in a cascade control mode, one being an internal current control and the other being an external voltage control. In this new approach, the voltage loop would provide a reference current to the current loop, which would control the converter's inductor's current and, therefore, the output voltage. A representation of this alternative method can be seen in Figure 4.8.

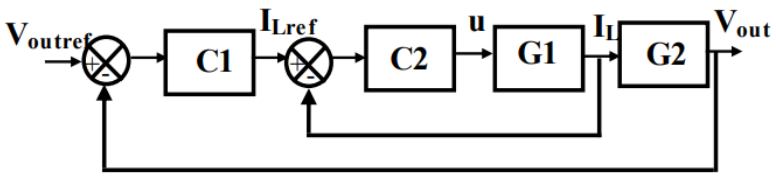

Figure 4.8: Cascade control block diagram [35]

In this block diagram, we have two control units (C1 and C2), that are both PI controllers, with their own proportional and integral terms. G1 and G2 are transfer functions that represents the mathematical relation between the transistor's duty-cycle and the inductor current of that converter and the mathematical relation between the inductor current and the output voltage of that converter.

One important requirement for the correct functioning of cascade controllers is that the inner current control loop needs to be at least 4 times faster than the outer voltage loop. This attests that the reference value given by the outer loop is seeing as a constant by the inner loop, which guarantees that the primary process is reacting, at a certain time, only to the primary controller [36].

Knowing all these concepts, a cascade control system was implemented on MATLAB/ Simulink to compare its responses with the ones of a simple PI control system. Both systems were used in order to control the output voltage of a Buck Converter with varying voltage reference, as we can see in Figure 4.9, showing the cascade control example.

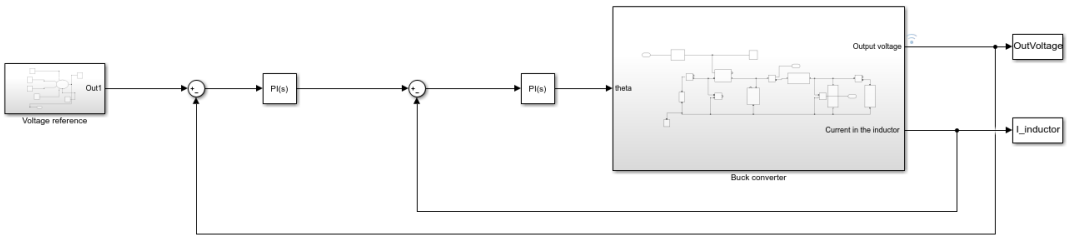

Figure 4.9: Cascade control system's implementation

The simulation's parameters are shown in the table below. The voltage reference used in the system varies from zero to 30 volts, as we will see in the simulations. As for the terms in the controllers, we will have, as we can see in Table 4.3, four. These are: the proportional and integral term for the voltage and current controller, noted as $K_{p,voltage}$, $K_{p,current}$, $K_{i,voltage}$ and $K_{i,current}$.

Table 4.3: Control parameters calculation scenario

Parameter	**Value**
Input voltage	100 V
Inductance	200 mH
Capacitance	100 μF
Load	100 Ω
Proportional control - voltage loop ($K_{p,voltage}$)	0.01
Integral control - voltage loop ($K_{i,voltage}$)	1
Proportional control - current loop ($K_{p,current}$)	8.4
Integral control - current loop ($K_{i,current}$)	8400

The results of these simulations are shown in figures 4.10, 4.11, 4.12 and 4.13. As we can see from figures 4.10 and 4.11, in the case of the cascade control system, the response to changes in the voltage reference is considerably fast and without much oscillation of both the output voltage and the current in the inductor. From these graphs, it is clear that, in fact, the dynamics of the current control loop are much faster than the dynamics of the voltage control loop, a requirement that was previously mentioned.

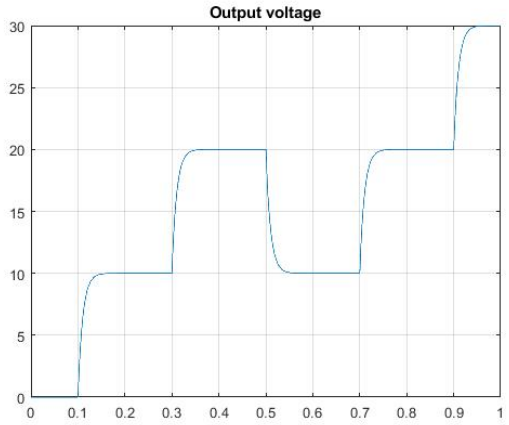

Figure 4.10: Buck Converter's output voltage - cascade control

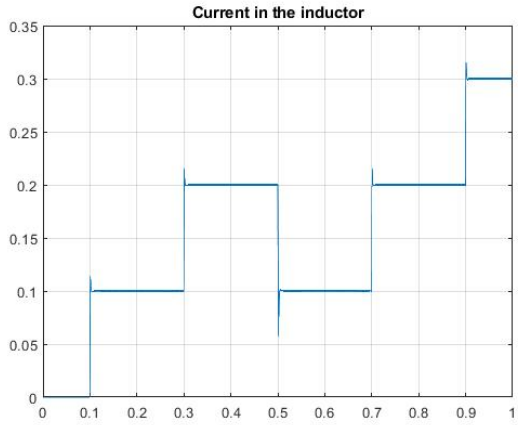

Figure 4.11: Buck Converter's inductor current - cascade control

As for the scenario where we used a simple feedback control system, we can see

that the responses were not as fast as the ones presented above and they showed considerable amount of oscillation. As expected, in this case, the dynamics of the current and voltage are the same, as there are no distinctions of inner and outer loops.

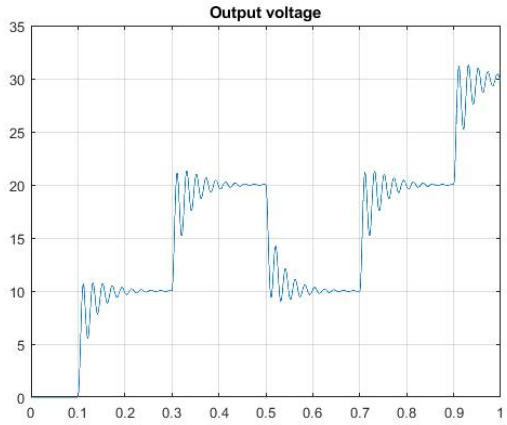

Figure 4.12: Buck Converter's output voltage - simple feedback control

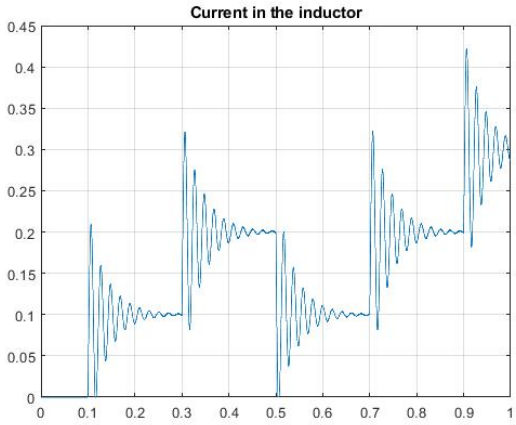

Figure 4.13: Buck Converter's inductor current - simple feedback control

Based on this comparison, it is clear that, indeed, the cascade control system shows advantages, when compared to simple feedback voltage control systems, as its responses, both in terms of voltage and current were faster and more stable. Because of this understanding, we will use, in this thesis, cascade control systems for all our DC-DC converters associated with loads.

Having decided that, it is important to understand how we can correctly set the $K_{p,voltage}$, $K_{p,current}$, $K_{i,voltage}$ and $K_{i,current}$ parameters of the control system, as they would vary from situation to situation, depending on both the input and output voltage, as well as the characteristics of the DC-DC converter that we will use. An investigation on this will be carried on the next section.

4.3 Tuning of Cascade Control

One of the central challenges that developers have when discussing controlled systems is about how to correctly set the control parameters, as they determine the efficiency with which the system adapts to new circumstances. In some studies about DC-DC converters, the parameters, for both control loops, are founded by

trial and error, as was the system described by Table 4.3, developed by [35].

Although this trial and error approach does work for some situations, as the complexity of the system increases, so does the challenges of not having a standardized methodology to calculate these parameters. With that in mind, in [37], an approach was developed to provide the control parameters of slightly modified cascade PI controllers. It is important to mention that, due to some small changes in the system, we are not dealing with the pure cascade control system (Figure 4.8), as we will show in this section.

In the mentioned paper ([37]), this control approach was developed for a Boost Converter. In this thesis we will show how it was done, as well as an extrapolation developed to use the same approach for a Buck converter.

4.3.1 Tuning of Buck Converter control system

The first step towards finding the control parameters of a Buck Converter, in this new approach, is to find its dynamic model, with state-space equations. The Buck Converter that we will use for it is shown in Figure 4.14.

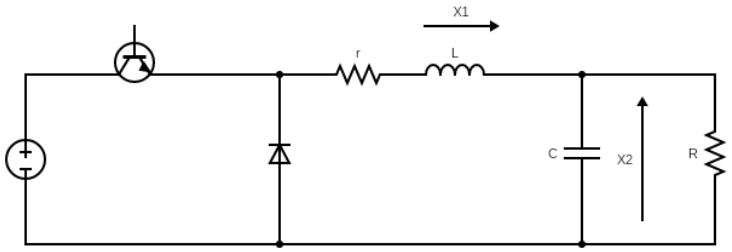

Figure 4.14: Buck converter used to dynamic modelling

In order to find its model, we need to think about the two distinct moments of the converter's operation: when the transistor is closed and when it is opened. In both, we need to find the nonlinear equations that describes the behaviour of the inductor's current (x_1) and capacitor's voltage (x_2), with respect to the parameters of the circuit, such as the input voltage (E), inductance (L), capacitance (C), parasitic resistance (r) and load (R).

Equation 4.1 shows the dynamic model of the converter when the transistor is closed (θ).

$$\begin{aligned} L.\dot{x_1} &= E - r.x_1 - x_2 \\ C.\dot{x_2} &= x_1 - \frac{x_2}{R} \end{aligned} \tag{4.1}$$

Equation 4.2 shows the dynamic model of the converter when the transistor is opened $(1 - \theta)$.

$$\begin{aligned} L.\dot{x_1} &= -r.x_1 - x_2 \\ C.\dot{x_2} &= x_1 - \frac{x_2}{R} \end{aligned} \tag{4.2}$$

Then, in order to find the global model of the circuit presented in Figure 4.14, we need to weight the above equations with respect to their amount of time, that is θ and $1 - \theta$. By doing this, we have as global equations of the converter:

$$\begin{aligned} L.\dot{x_1} &= E.\theta - r.x_1 - x_2 \\ C.\dot{x_2} &= x_1 - \frac{x_2}{R} \end{aligned} \tag{4.3}$$

Those two equations represent the current and voltage dynamics, respectively, as x_1 is the representation of the current in the converter's inductor and x_2 of its output voltage.

Having them, the next step would be to find an equations that would represent the inner current loop, that is, an equation that, from the difference between the reference current and the actual measured current in the inductor, would provide us the duty-cycle value, our control signal. To find it, we need first to define an equation for the duty-cycle that would decouple the two loops, eliminating, then, the x_2 signal from the current equation of 4.3. This equation will be:

$$\theta = \frac{x_2}{E} + e_{x1}.PI_{controller} \tag{4.4}$$

With e_{x1} being the error gotten from the reference current and the actual measured current $(x_{1,ref} - x_1)$.

As we can see, if we add Equation 4.4 on the first equation of the model 4.3, we would be able to cancel the x_2 parameter of that equation, as follows:

$$
\begin{aligned}
L.\dot{x_1} &= E.\theta - r.x_1 - x_2 \\
L.\dot{x_1} &= E.(\frac{x_2}{E} + e_{x1}.PI_{controller}) - r.x_1 - x_2 \\
L.\dot{x_1} &= E.\frac{x_2}{E} + E.e_{x1}.PI_{controller} - r.x_1 - x_2 \\
L.\dot{x_1} &= E.e_{x1}.PI_{controller} - r._{x1}
\end{aligned}
\tag{4.5}
$$

By implementing the error and adding the contribution of the PI controller to it, we will have a complete equation for the duty-cycle as follows:

$$\theta = \frac{x_2}{E} + K_{p,current}.(x_{1,ref} - x_1) + K_{i,current}.\int(x_{1,ref} - x_1)dt \tag{4.6}$$

By adding this to the current equation of 4.3, we will have the decoupled equation that represents the current loop control:

$$L.\dot{x_1} = E.K_{p,current}.(x_{1,ref} - x_1) + E.K_{i,current}.\int(x_{1,ref} - x_1)dt - r.x_1 \tag{4.7}$$

From this equation, we can find the relation between the current in the inductor and the reference current given by the outer loop. For that, we need to apply the Laplace transform to equation 4.7 and isolate its terms. By doing that, we will find:

$$\frac{X_1}{X_{1,ref}}(s) = \frac{E.K_{p,current}.s + E.K_{i,current}}{L.s^2 + (E.K_{p,current} + r).s + E.K_{i,current}} \tag{4.8}$$

The central idea of this tuning approach is that we will set the parameters $K_{p,current}$ and $K_{i,current}$ in a way that the equation 4.8 would represent a first order system, with a specific time constant ($\tau_{current}$), defined by the user. First order systems have the following transfer function:

$$\frac{X_1}{X_{1,ref}}(s) = \frac{1}{\tau_{current}.s + 1} \tag{4.9}$$

It is crucial to understand that, having defined the converter's parameters, such as its input voltage, inductance and the inductor's parasitic resistance, there is just one pair of $K_{p,current}$ and $K_{i,current}$ that allows this system to have a first order transfer function with the user defined time constant ($\tau_{current}$). After doing some calculations, we can conclude that this pair of parameters will be:

$$
\begin{aligned}
K_{p,current} &= \frac{L}{E.\tau_{current}} \\
K_{i,current} &= \frac{-r}{E.\tau_{current}}
\end{aligned}
\tag{4.10}
$$

This already gives us an approach to correctly set two out of the four control parameters, based on a set of pre-defined conditions, as the time constant for the current loop and the converter's components values. For the outer voltage loop, a similar approach is carried.

In this case, we do not need to set a new relation, as we did in 4.6, in order to make the voltage equation of our model independent to the current. As we know, in cascade control system the reference value for the inner loop control variable is given by the outer loop control (Figure 4.8) and, as the inner loop is much faster than the outer loop, we can assume, when analyzing the outer loop, that the value of the inductor's current will be the same as the reference given to it. Also, we know that the reference given to it, in here, will be the result of the error function of the outer loop after a PI controller, that is:

$$x_1 = K_{p,voltage}.(x_{2,ref} - x_2) + K_{i,voltage}.\int (x_{2,ref} - x_2)dt \tag{4.11}$$

Adding this equation to the one related to the output voltage of 4.3, we can have the decoupled equation for the voltage loop, as it is shown below:

$$C.\dot{x_2} = K_{p,voltage}.(x_{2,ref} - x_2) + K_{i,voltage}.\int (x_{2,ref} - x_2)dt - \frac{x_2}{R} \tag{4.12}$$

Following the same steps of the current loop, we need to get the Laplace transfer function between the output voltage and the reference voltage, that is:

$$\frac{X_2}{X_{2,ref}}(s) = \frac{K_{p,voltage}.s + K_{i,voltage}}{C.s^2 + (K_{p,voltage} + \frac{1}{R}).s + K_{i,voltage}} \tag{4.13}$$

As well as in the current loop, the idea of this tuning method is to set the control parameters $K_{p,voltage}$ and $K_{i,voltage}$ in a way that the above equation would become a first order one, with a time constant $\tau_{voltage}$ pre-defined. After doing some careful calculations, it was found that the only combination of parameters that guaranteed this was:

$$\begin{aligned} K_{p,voltage} &= \frac{C}{\tau_{voltage}} \\ K_{i,voltage} &= \frac{1}{R.\tau_{voltage}} \end{aligned} \tag{4.14}$$

One of the most interesting characteristics of this approach is that the selection of the system's time constant is a job for the developer and, with this, a central requirement can be respected: the inner loop needs to be at least 4 times faster

than the outer one, for the cascade control system to work properly.

As mentioned before, this approach would provide minor changes in the common cascade control block diagram (presented in Figure 4.8). This happens because, as we saw in equation 4.6, we do not have a simple PI controller from the error signal to the duty-cycle in the inner loop, but we have a combination of a PI controller and a term that is dependent on the output and input voltages. Finally, the block diagram for the Buck Converter control that will be used in this thesis is provided below:

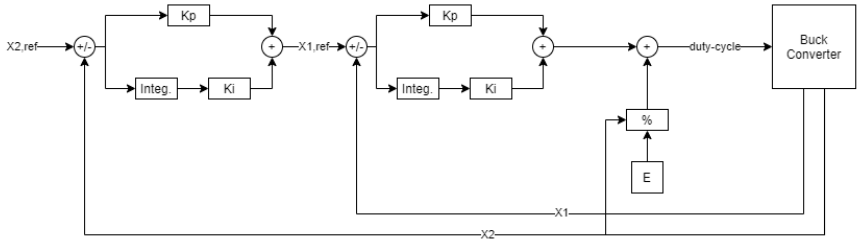

Figure 4.15: Alternative Buck Converter's cascade controller

In the above scheme, the operation % is not the module operator, but a divider, as, in Equation 4.6, we have the output voltage divided by the input voltage in order to decouple the inner loop. This symbol was used in the lack of the correct one.

4.3.2 Tuning of Boost Converter control system

As for the Boost Converter, the approach will be similar. The first thing we need to do is to define a circuit that our dynamic model will be based on. The proposed circuit is shown below:

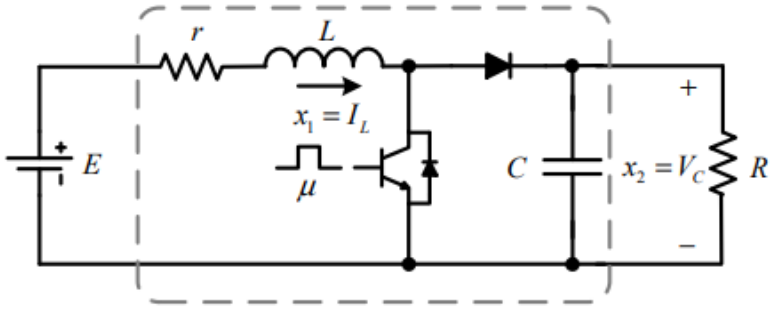

Figure 4.16: Boost converter used for the dynamic modelling [37]

To model this converter, we will take into account the differential equations of both its inductor and output capacitor in two scenarios, when the transistor is ON and when it is OFF. Based on the duty-cycle (θ) of the transistor, we will weight the scenarios, finding a complete model, that is shown below.

$$\begin{aligned} L.\dot{x_1} &= -r.x_1 - (1-\theta).x_2 + E \\ C.\dot{x_2} &= (1-\theta).x_1 - \frac{x_2}{R} \end{aligned} \tag{4.15}$$

Where x_1 is the inductor current, x_2 is the capacitor's voltage and E is the DC input voltage. The converter inductance and capacitance are given by L and C and R is the resistive load. For experimental application the inductor's parasitic resistance (r) is taken into account in our modelling.

The idea, then, is to provide a duty-cycle equation, considering both control parameters of the inner loop ($K_{p,current}$ and $K_{i,current}$), in a way to decouple the inner and outer loops of our system, which means making the first equation of 4.15 not dependent on the output voltage (x_2). This can be done by defining the following equation for the duty-cycle:

$$\theta = 1 + \frac{1}{x_2}.(K_{p,current}(x_{1,ref} - x_1) + K_{i,current}\int(x_{1,ref} - x_1)dt) \tag{4.16}$$

Using this relation on the inductor's current from our dynamic model 4.15, we have the decouple equation for the inner loop:

$$L.\dot{x_1} = -(r + K_{p,current})x_1 + K_{i,current}(\int(x_{1,ref} - x_1)dt) + E + K_{p,current}.x_{1,ref} \tag{4.17}$$

Then, as done for the Buck Converter, we need to find the transfer function between the actual inductor's current (x_1) and its reference value ($x_{1,ref}$). To do that, we will apply the Laplace transform on the above equation, getting:

$$\frac{X_1}{X_{1,ref}}(s) = \frac{K_{p,current}.s + K_{i,current}}{L.s^2 + (r + K_{p,current}).s + K_{i,current}} \tag{4.18}$$

Then, as mentioned before, we need to find the control parameters of the inner loop ($K_{p,current}$ and $K_{i,current}$) in order to make this transfer function a first order one, with a pre-defined time constant ($\tau_{current}$). After performing the needed calculations, we can see that the control parameters are:

$$
\begin{aligned}
K_{p,current} &= \frac{L}{\tau_{current}} \\
K_{i,current} &= \frac{r}{\tau_{current}}
\end{aligned}
\tag{4.19}
$$

Differently from what was done for the Buck Converter, in here a change of variable was proposed for the voltage loop, in order to make the calculations easier to do. For that, instead of using the output voltage (x_2) in our modeling of the control, we will use the square of that value ($y = x_2^2$). After doing this change in variables, we need to define a second differential equation to represent the outer voltage control loop and, on [37], the following equation was proposed.

$$
C\dot{y} = -\frac{2}{R}.y + 2.E.x_1 \tag{4.20}
$$

Then, we need to find a transfer function of this differential equation and consider that the inductor's current will assume a value that is equal to the error of y ($y_{ref} - y$) processed by the PI controller of the outer loop, as done in Equation 4.11 for the Buck Converter. After applying the Laplace transform in the result, we have:

$$
\frac{Y}{Y_{ref}}(s) = \frac{2.E.K_{p,voltage}.s + 2.E.K_{i,voltage}}{C.s^2 + (\frac{2}{R} + 2.E.K_{p,voltage}).s + 2.E.K_{i,voltage}} \tag{4.21}
$$

Again, the idea is to chose the correct values for the control parameters ($K_{p,voltage}$ and $K_{i,voltage}$) in order to make that transfer function a first order one, with a pre-defined time constant ($\tau_{voltage}$). The control parameters that allow this to be true are shown below:

$$
\begin{aligned}
K_{p,voltage} &= \frac{C}{2.E.\tau_{voltage}} \\
K_{i,voltage} &= \frac{1}{E.R.\tau_{voltage}}
\end{aligned}
\tag{4.22}
$$

Again, as we can see from equations 4.19 and 4.22, the control parameters are dependent on the system's parameters, such as the inductor, capacitor, inductor's resistive impedance and input voltage, as well as two pre-defined time constants. It is important to remember that the internal loop needs to be at least 4 times faster than the voltage loop, in order for it to see the current reference as a constant and guarantee the proper work of the controller.

Once again, the final block diagram for this control system will not be exactly like the usual cascade control diagram (Figure 4.8), but an alternative that allows the easy tuning of its control parameters. The new block diagram is shown below, with the % representation being the division operator, due to the lack of a better symbol.

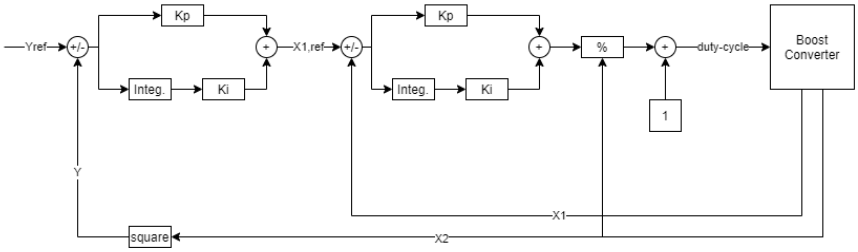

Figure 4.17: Alternative Boost Converter's cascade controller

Having defined the control strategy that we will use for our DC-DC converters, we can now start discussing the model that was developed for the DC Microgrid. On the next chapter, each of its main components are described and, on Chapter 6, its results are carefully discussed.

Chapter 5

Microgrid's model description

Having decided for which DC-DC converters we will use, as well as which control approach, we can start to describe the microgrid model that will be the core of this study. This model is constituted mainly of 4 parts:

- Generation units
- Storage unit
- DC-DC converters
- Loads

The generation units are responsible for providing the power that will be consumed by the loads and are constituted of two renewable energy sources: PV and wind. As for the storage unit, we have a battery that is responsible to maintain a steady voltage at the main bus, and it does that with the help of a bidirectional converter. This bidirectional converter supplies power from the battery to the bus when the loads are requiring more than the generation units are providing (discharging the battery) or providing power to the battery when the generation units are providing more than what the loads are requiring (charging the battery). We have, also, DC-DC converters connecting the main bus to the loads, adapting the voltage level to meet their requirements, with the help of the alternative cascade controllers from Chapter 4.

A high-level overview of the model used can be seen in the figure below:

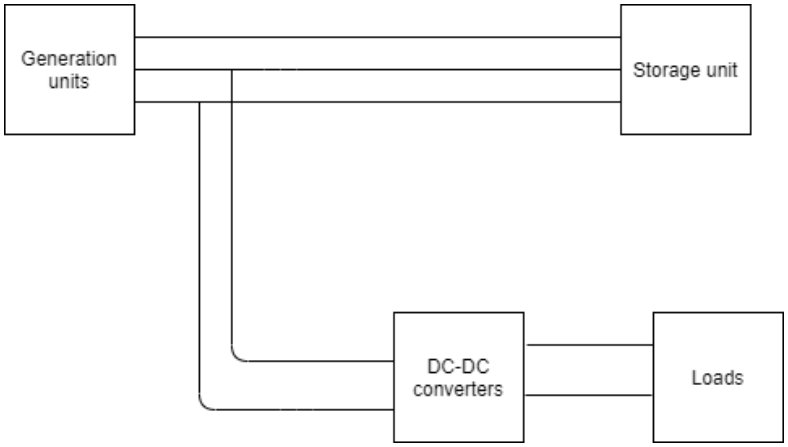

Figure 5.1: Model overview

One important characteristics of the microgrid model that was developed is that it constitutes a bipolar DC microgrid, which means that the main busbar, that connects the generations units to the storage unit, works in a three-wire system, as we can see in Figure 5.1. This bipolar characteristics means that the system will have three main wires associated with three different voltages (V_{DC}, $-V_{DC}$ and neutral line), providing, then, three input voltage connection options to the customers (V_{DC}, $-V_{DC}$ and $2V_{DC}$), increasing the systems flexibility. Also, having a bipolar system is a good advantage in fault situations, because, if we have a fault in one of the DC poles, power can still be supplied by the two other wires. Therefore, in bipolar systems, the reliability, availability and power quality of the system are increased during fault conditions [38].

In the following sections we will deep dive in each of the four main parts of the model, describing how they should operate and how they were developed.

5.1 Generation units

As mentioned, we have in our model two main power sources: PV and wind energy. They are responsible for providing all the energy to the system, as our microgrid is isolated from the main grid. Because of the characteristics of the generation units used, environmental informations were needed to our design, such as the irradiance and temperature that we have in the installation point of the PV panels, as well as the wind speed for the wind generation. The weather informations were found, for a site near Louvain-la-Neuve, Belgium, on [39] and [40].

We will discuss the two generation units individually below.

5.1.1 PV generation

For the PV generation, we used the PV array block from MATLAB/ Simulink, that has, as inputs, the irradiance and temperature of the installation site. This PV array used in the simulations has the characteristics provided in the table below:

Table 5.1: Parameters of PV array

Parameter	**Parameter Value**
Number of strings that are connected in parallel	5
Number of PV modules connected in series in each string	1
Module maximum power	213,15 W
Cells per module	60
Open circuit voltage	36,3 V
Short circuit current	7,84 A

As we know, the operation of PV panels is strongly related to its I-V curve, that relates the current and voltage across its terminals. In this relation, we have three main points of operation that are important to consider, two of them already presented on Table 5.1, that are the open circuit voltage, when the current is zero, and the short circuit current, when the voltage is zero. The third point would be the maximum power point (MPP), where the multiplication of the current and voltage provides to us the biggest power to be consumed. The I-V curves of the used PV array, for three different temperatures, are shown below:

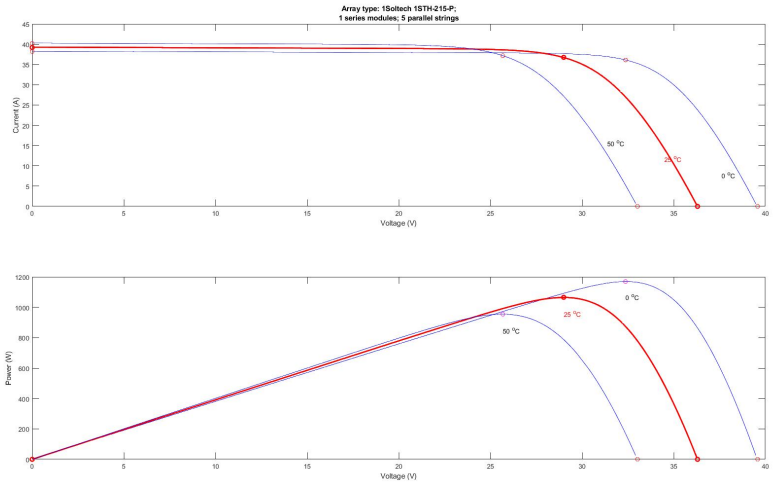

Figure 5.2: PV panel's I-V and power relations

From this curve it is clear that we need to ensure that the PV array works in the maximum power point, in order to offer to the circuit the biggest amount of power possible. The search for this operating point is called maximum power point tracking (MPPT), as it was described in [41], and the way that was chosen to perform this was through the usage of a Boost Converter, with a perturb and observe (P&O) algorithm to set the transistor's duty-cycle.

What this algorithm does is to continuously increase the duty-cycle of the transistor, from a near-zero value and, after every step, it measures the output power until it stops increasing. When it reaches this maximum power point, it continues to measure the power for a duty-cycle slightly bigger or smaller, therefore being able to adapt to different conditions of the system, that could require a different I-V relation for a maximum power point.

The MATLAB/ Simulink model of the PV array and the Boost Converter, as well as the control unit, is shown below:

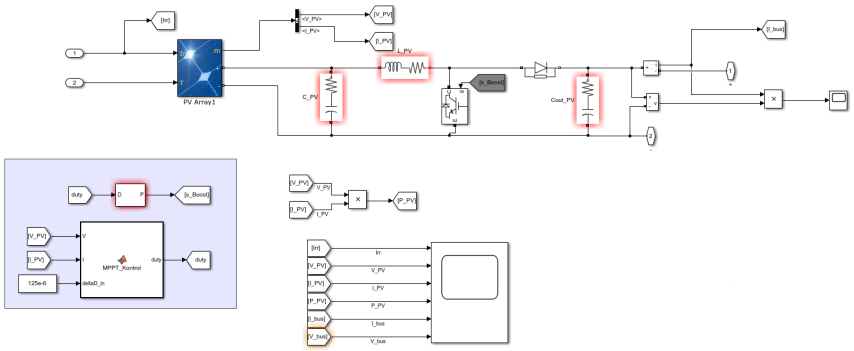

Figure 5.3: Model of PV array with MPPT

5.1.2 Wind generation

As for the wind generation, we used the Wind Turbine block from MATLAB/ Simulink, with one input: the wind speed of the installation site. Associate with this turbine, we had a permanent magnet synchronous machine, that was working as a generator for our model. The main characteristics of these two blocks are shown below:

Table 5.2: Parameters of wind generation

Parameter	Parameter Value
Nominal mechanical output power	1.5 MW
Stator phase resistance	0.425 Ω
Armature inductance	0.395 mH
Flux linkage	0.433 V.s

It is important to notice that the permanent magnet synchronous machine works on 3-phase configuration and, therefore, we need to have a rectifier in its output, in order to have a DC voltage level.

In wind turbines, as well as for PV panels, we need to develop a control method that would guarantee that we are working on the maximum power point of the turbine. We can use, after the rectifier, the same MPPT strategy used in the PV panels, that is, the perturb and observe (P&O) algorithm to set the duty-cycle of a Boost converter. This approach was discussed in [42] and a model of the strategy is shown below:

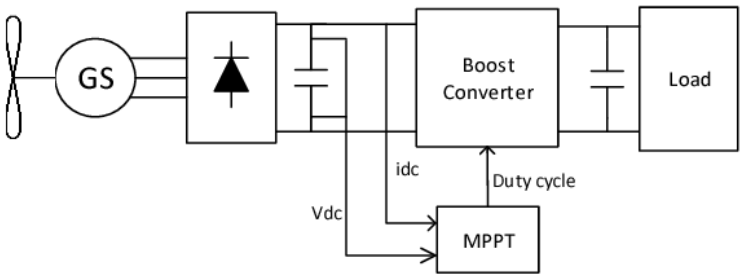

Figure 5.4: Control strategy of Wind Turbine [42]

As mentioned for the PV panels, the P&O algorithm work by changing the control parameter and observe the output change. The advantages of this algorithm is that it has low complexity, high efficiency and does not require several sensors to be performed [42].

The implemented MATLAB/ Simulink model is shown in Figure 5.5, a system that was based on the model presented by [42] on Figure 5.4.

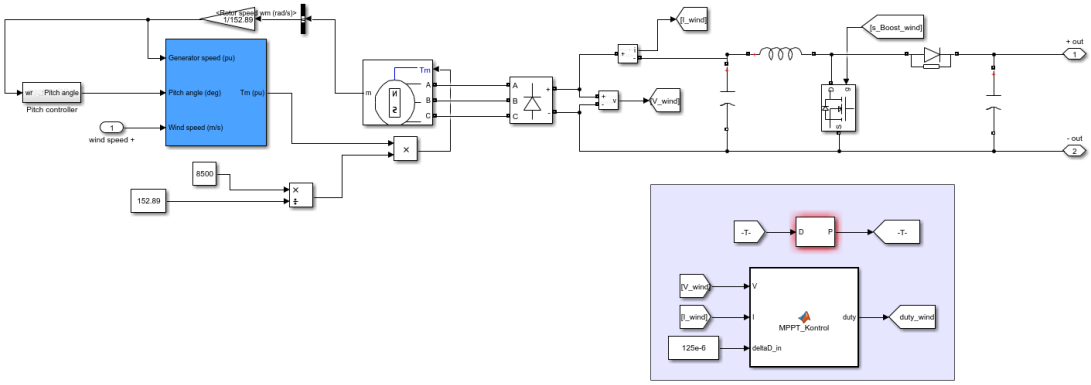

Figure 5.5: Wind generation with MPPT

5.2 Storage unit

As for the second main part of the DC Microgrid model, the storage unit, we are using a lithium-Ion battery associated with a bidirectional DC-DC converter, as mentioned before. The idea of this unit is that it will fixate the voltage levels of the main busbar, providing energy to it when the generation units are not generating the needed energy required by the loads and absorbing energy when they are providing more energy than the required.

The way to do that is through the usage of bidirectional converters, a type of converter that can work as a Boost converter at some situations and as a Buck converter in others, being able, then, to step up and down the voltage level of a given busbar. This converter can be seen in Figure 5.6, where on its right hand side we have the Lithium-Ion battery used and on its left hand side we have the main busbar, where the generation units and loads are connected.

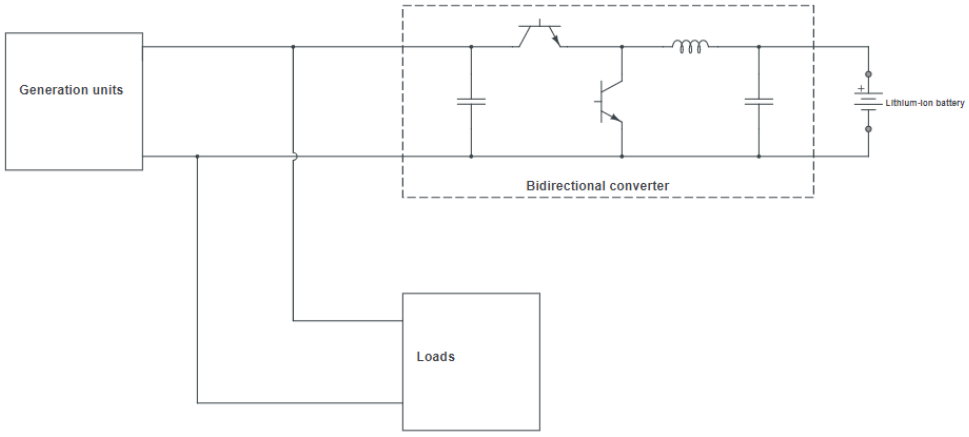

Figure 5.6: Battery's Bidirectional converter

We can see in the table below the main parameters of the Lithium-Ion battery and the bidirectional converter.

Table 5.3: Battery and bidirectional converter parameters

Parameter	**Parameter Value**
Battery nominal voltage	120V
Battery rated capacity	10 Ah
Battery initial state-of-charge (SOC)	50 %
Battery response time	0.01s
Converter's capacitors	110 μF
Converter's inductor	0.01 μH
Busbar voltage reference (Vref)	150V
Proportional parameter - Boost operation ($K_{p,boost}$)	0.02
Integral parameter - Boost operation ($K_{i,boost}$)	3
Proportional parameter - Buck operation ($K_{p,buck}$)	0.02
Integral parameter - Buck operation ($K_{i,buck}$)	110

Differently from the main converters, associated with the loads, we will not use in here a complex control method as described in Chapter 4. As we can see from the circuit in Figure 5.6, we have two transistors to control, with two different duty-cycles. One of the transistors would be associated with the Boost operating mode, when $V_{ref} > V_{bus}$, and the other with the Buck operation mode, when $V_{ref} < V_{bus}$. That way, when one is operating ($\theta \neq 0$), the other one is not ($\theta = 0$). That being said, we need to do two things in the control unit of these converters: check if the voltage in the bus is bigger or smaller than the reference and calculate the corresponding duty-cycles of the transistors, what we will do through two PI controller, with pre-defined control parameters. The control unit of this converter can be seen in the figure below, extracted from our model on MATLAB/ Simulink.

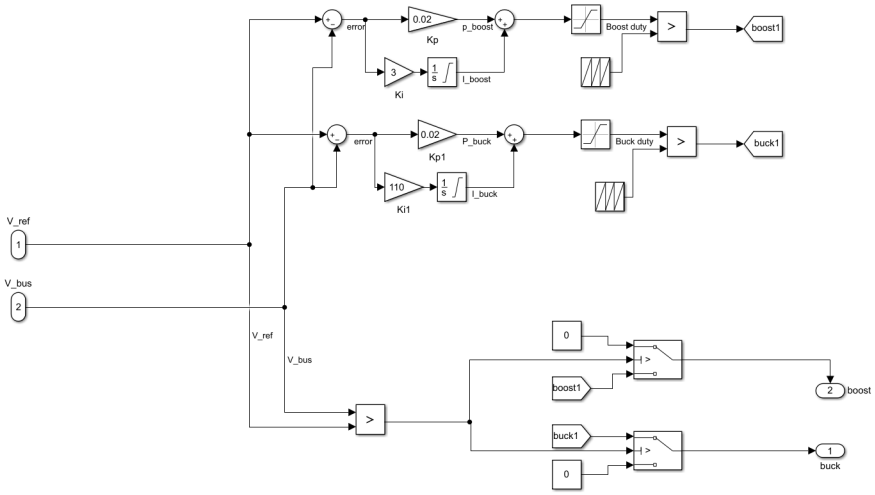

Figure 5.7: Control unit of the bidirectional converter

As we can see in the bottom part of the circuit, when one transistor is operating, the other is not. In the top part, we have, as mentioned, a simple PI controller that will provide the duty-cycles, name here boost1 and buck1, for the transistors.

Finally, it is important to mention that, in order to have a bipolar microgrid, aiming at the advantages already mentioned, we need to provide not only the positive voltage level ($+V_{DC}$) but the negative one ($-V_{DC}$) as well. Because of this, we need to have two bidirectional converter-battery systems, one to fixate the voltage level between the neutral line and the positive voltage level and another between the negative voltage level and the neutral line. In both, the parameters described in the Table 5.3 were used.

The model used in the storage unit is shown in the figure below, where we can clearly see the two bidirectional converter-battery systems, each with their controller, working.

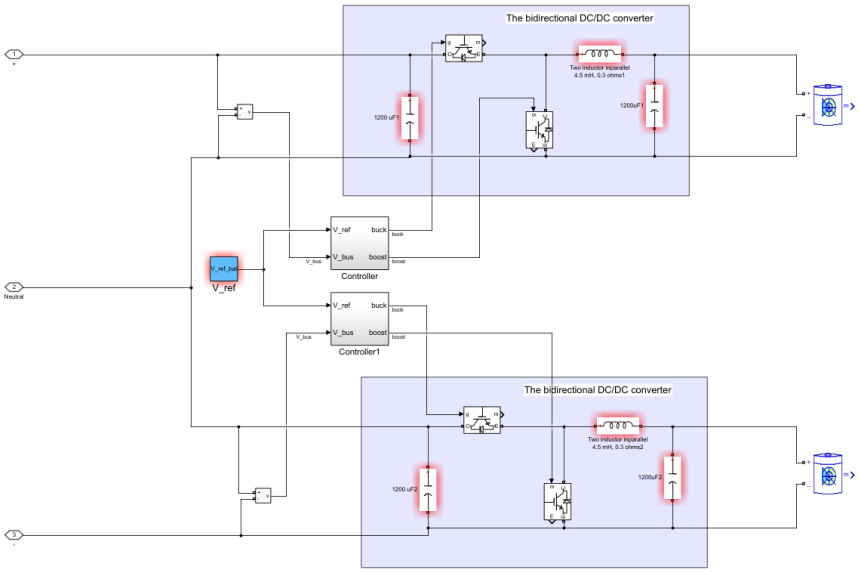

Figure 5.8: MATLAB/ Simulink storage units model (Batteries + bidirectional converters)

5.3 DC-DC Power Converters

As for the third part of the model, the power converters, their importance rely on the fact that we need to adapt the voltage level from the main busbar to the loads, in order to meet with their requirements. In our model, we have five groups of loads, four representations of residential loads and one of a high-voltage site.

For the high-voltage site, we have a Boost Converter connected between the positive and negative wires on the main busbar (300V input voltage), stepping up the voltage level to 650V in order to feed the load. For the residential loads, we used Boost and Buck converters connected in series to allow the provision of all voltage levels required. For all these loads, we used, as input voltage of the Boost converters, 150V (either from $-V_{DC}$ to neutral or from neutral to $+V_{DC}$). A representation of the described structure can be seen in the Figure 5.9

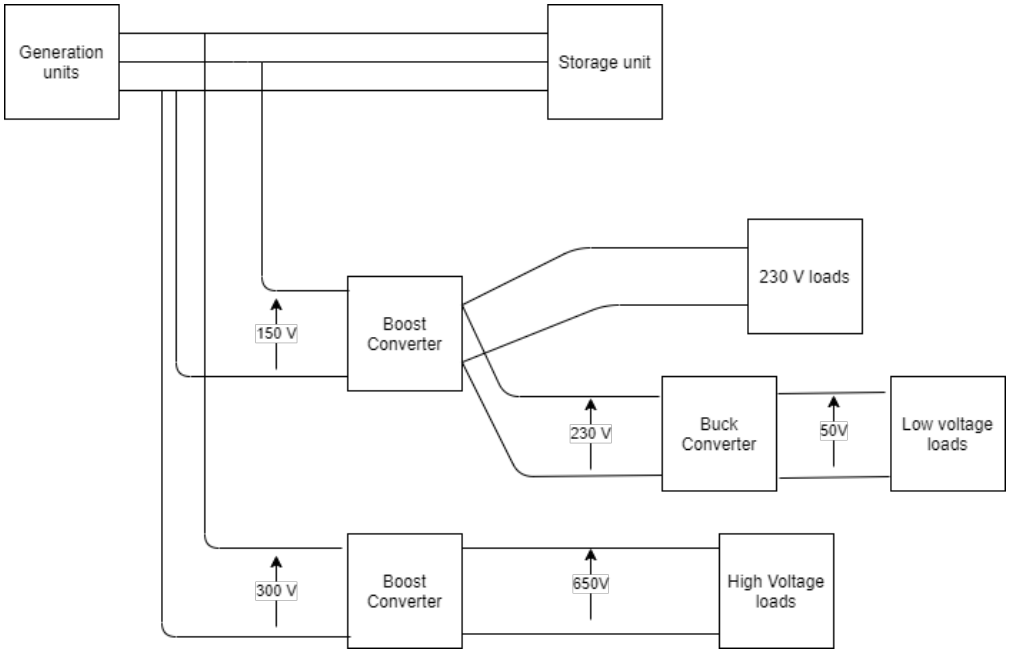

Figure 5.9: Model overview - power converters strategy

As we know from [43], a short to medium transmission line (length until 80 km) can be modelled as a resistance in series with an inductance. Because of this, a choice was made in this study to use only Boost converters connected to transmission lines and, if there was a need to reduce the voltage level of the Boost's output, we would add a Buck Converter in series with it, before connecting the load. That choice brings an interesting simplification to our model, as the Boost's control strategy defined could incorporate the transmission line to the converter's inductor and its parasitic resistance, that are connected directly to the voltage source, as shown in Figure 4.16. Due to this, we could analyze the system transmission line + converter as a simple modified converter, with bigger inductance and parasitic resistance, as shown in the figure below:

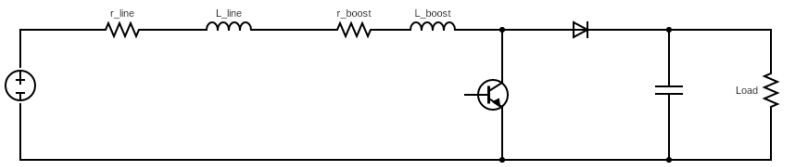

Figure 5.10: Transmission line incorporated to Boost Converter

In terms of equations, we would need to adjust, then, the converter's parasitic

resistance and the inductance in order to find its parameters for the control loop (4.19) of its control. This can be seen in the following equations:

$$\begin{aligned} L_{control} &= L_{line} + L_{boost} \\ r_{control} &= r_{line} + r_{boost} \\ K_{p,voltage} &= \frac{C}{2.E.\tau_{voltage}} \\ K_{i,voltage} &= \frac{1}{E.R.\tau_{voltage}} \\ K_{p,current} &= \frac{L_{control}}{\tau_{current}} \\ K_{i,current} &= \frac{r_{control}}{\tau_{current}} \end{aligned} \tag{5.1}$$

It is important to reinforce why the same could not be done by connecting a Buck Converter directly to the transmission line. As we know from Figure 4.14, directly connected to the voltage source, in a Buck Converter, we have the transistor, and not the inductor. For that reason, adding the contribution of the transmission line to the converter's model would mean making bigger changes to Equation 4.3, as in this case we could not just add the inductances and the resistances, such as did in the equation above. For this reason, once again, we decided to use always, from the main busbar to the input of the load groups (houses), Boost converters and, for the loads that required smaller voltage levels, we added in series Buck converters to adapt it.

In our model, as we will discuss later, several converters, transmission lines and loads were used. In the table below, as an example, we will show the parameters for one of the Boost converters, already incorporating the transmission line in its circuit. As we can see, the control parameters incorporate the transmission line, as mentioned in equations 5.1.

Table 5.4: Line and converter parameters to set control parameters

Parameter	**Parameter Value**	**Parameter**	**Parameter Value**
Line length	1000 meters	Input voltage of Boost Converter	150V
Line resistance per km	73 m Ω	$\tau_{current}$	1 ms
Line inductance per km	0.92 mH	$\tau_{voltage}$	50 ms
Line resistance	73 m Ω	Load	145 Ω
Line inductance	0.92 mH	$K_{p,current}$	200.92
Parasitic resistance of Boost Converter	0.1 Ω	$K_{i,current}$	173
Inductance of Boost Converter	200 mH	$K_{p,voltage}$	$5.4.10^{-4}$
Capacitance of Boost Converter	8.2 mF	$K_{i,voltage}$	$9.2.10^{-4}$

Another thing that is interesting to understand is that, as we saw in equation 4.22, in order to correctly control the Boost Converter's voltage, we need to know the resistance of its load or, at least, an approximation of that. This is very simple when we have a single converter, but gets harder when we have converters working in series, as we will. As shown in Figure 5.9, the Boost converters will have in their outputs some loads connected, but, as well, some Buck Converters, in order to connect low voltage loads to it. Because of this we need to know the impedance of the Buck's load, not on its output, but a reflection of it to its input, in order to get the output equivalent resistance of the Boost converter output side. This can be easily done by understanding the correct working principle of the Buck converter, that, as mentioned in Chapter 2, steps-down the voltage level by stepping up the current. With this we can find the input impedance of a Buck converter as follows:

$$\begin{aligned} V_{out} &= V_{in}.\theta \\ I_{in} &= I_{out}.\theta \\ R_{in} &= \frac{V_{in}}{I_{in}} = \frac{V_{out}}{I_{out}.\theta^2} \\ R_{in} &= \frac{R_{out}}{\theta^2} \end{aligned} \tag{5.2}$$

To sum up, in order to have the Buck Converter's load reflected to its primary side, we need to get its output resistance and divide that value by the square of the Buck's transistor's duty-cycle.

Because the control strategy of the Boost Converter takes into account the load resistance connected to it, as seen in equation 4.22, we decided to separate the loads into two groups: big loads (small resistances) and small loads (big resistances). By avoiding the mixture of these two load types, we can guarantee that each Boost Converter's control is considering their loads, without one load dazzling another. This is important because, when we were using only one converter, we would have several loads in parallel in its output, having from small to big resistances, and, as a result, big resistances were being shadowed by small resistances and their resulting voltage response of the control system was not satisfactory enough. This problem was solved by separating the loads into groups of small resistances (such as EV chargers), medium resistances (such as air-conditioners) and big resistances (such as computers).

A representation of this arrangement is shown in Figure 5.11, where we have three Boost converters working in parallel, one per group of loads. By doing this, we were able to have more voltage levels available for our loads, as each Boost Converter could step-up their 150V input voltage to a different voltage level, in this example 450V for the EV charger, 400V for the air-conditioner and 230V for the small loads (which could have a series Buck Converter to reduce it, as mentioned below).

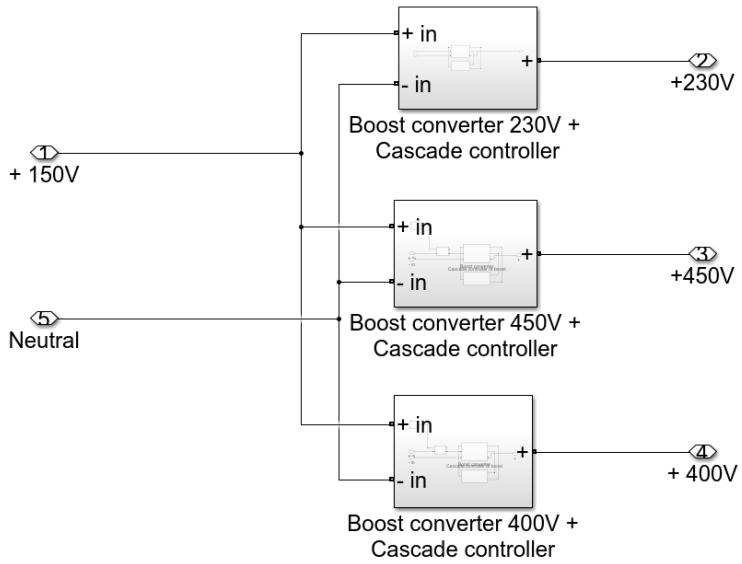

Figure 5.11: Three different Boost converter to three different load types

In the next image, we will show the second layer of converters that we had for the smaller loads. In it, we have three different resistances, representing a

phone, computer and a fridge, with the first two having voltage level requirements smaller than the 230V that we had in the output of the previously mentioned Boost Converter and the third one operating at 230V. Because of this, the first two loads required a new conversion and, for that, we added one Buck Converter for each, to go from 230V voltage level to 20 and 40V, respectively.

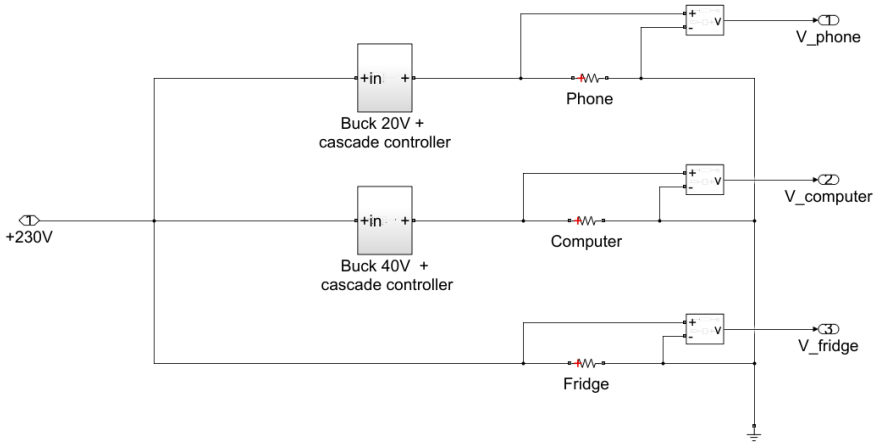

Figure 5.12: Buck converters connected in the output of Boost converters

5.4 Loads

Finally, for the last part of the model, we have the loads. The way that we structured the model was by grouping some loads in small house models, with resistances being connected and disconnected to the main grid, simulating electrical devices being turned ON and OFF. In our model, we have 4 houses, two connected between V_{DC} and neutral and two between $-V_{DC}$ and neutral, through transmission lines and Boost converters, as mentioned in the last section, and one high voltage resistive load, connected between $-V_{DC}$ and V_{DC}.

All loads are purely resistive and represent a typical device in everyone's household, like computers, cellphones, showers and others. The houses were classified into primary and secondary, based on the connection point that they used, that is, from the main busbar to a primary house, we would have one transmission line and, for a secondary house, we would have two transmission lines, one to go from the main busbar to the first house and another one between houses. This was done to simulate a neighbourhood, where you have transmission lines between neighbour houses to connect them.

In the table below we can see a description of all the loads used:

Table 5.5: Load parameters used in the model

House	**Load**	**Voltage level (V)**	**Resistance (Ω)**
House 1 (Primary)	Phone	20	100
	Computer	40	200
	Fridge	230	150
	EV charger	450	3,6
	Air-conditioner	400	80
House 2 (Secondary)	Phone	30	130
	Computer	50	180
	Fridge	230	130
	Shower	230	5,8
	House heater	230	8,82
House 3 (Primary)	Phone	45	170
	Computer	70	210
	Fridge	230	100
House 4 (Secondary)	Phone	30	130
	Computer	50	180
	Fridge	230	130
	Shower	230	5,8
	Heater	230	8,82
High voltage site (Primary)	HV load	650	5,8

The resistances and voltage levels shown in the above table were found in datasheets, available online, of typical electrical devices. With the exception of the fridge ones, all loads were turned ON and OFF repeatedly in our simulations, as we will see in the next chapter, and their voltage were controlled by systems such as the described in Chapter 4.

Before jumping to the next chapter, where we will show and discuss the main results found, we will provide the MATLAB/ Simulink diagram of the model developed. In this model, shown in Figure 5.13, we can clearly see the generation units block, with irradiance, temperature and wind speed as inputs, the storage system that is used to fixate the voltage levels of the bipolar busbar and all the loads, connected through transmission lines, both primary and secondary, and Boost converters, represented inside four houses and one high voltage site.

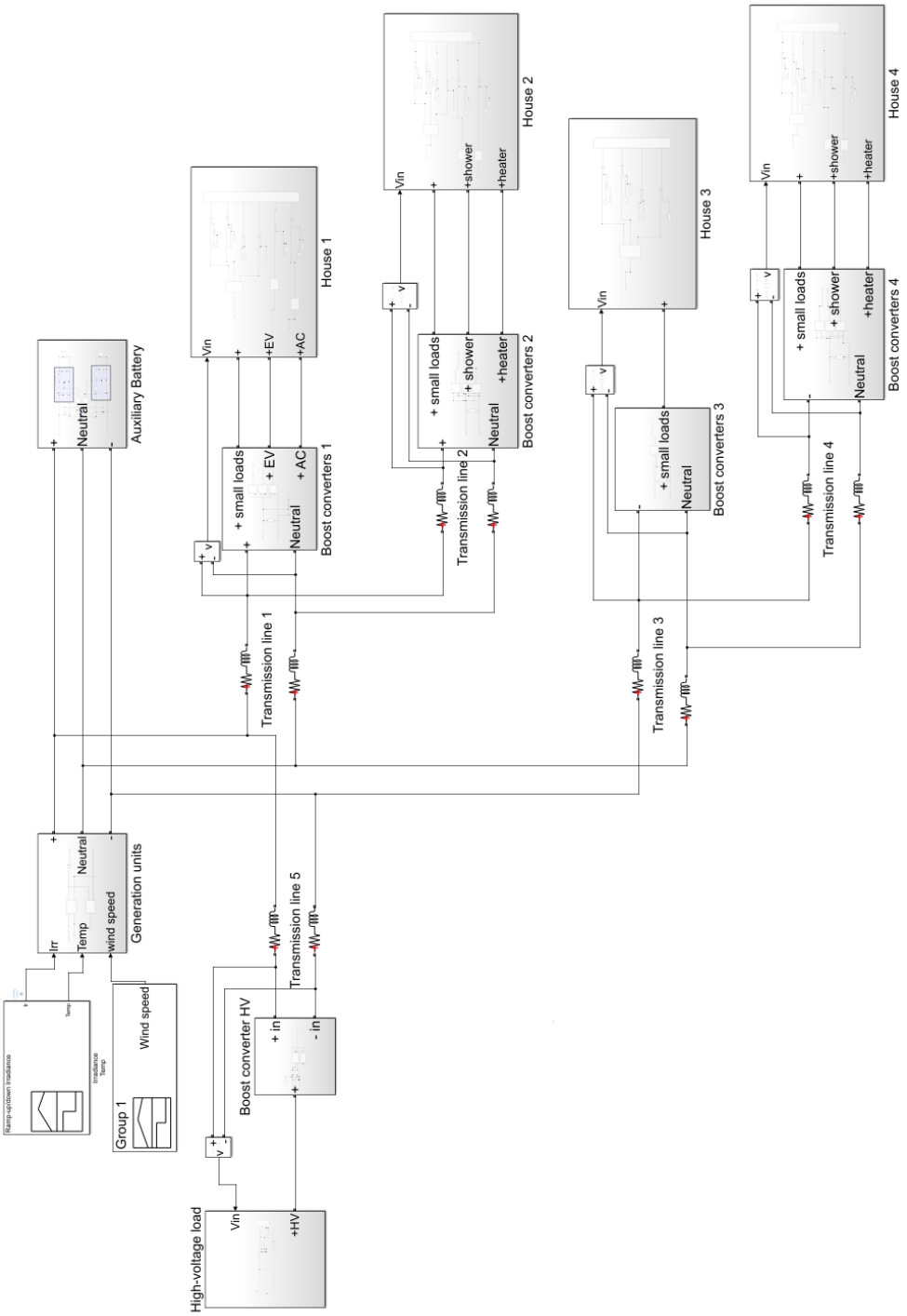

Figure 5.13: Model developed on MATLAB/ Simulink

In the next chapter, we will discuss all the results found in our simulation. We will focus on the voltage levels, both in the main busbar and in the loads end, showing that the control system for both the Boost and the Buck converter, described in Chapter 4, worked properly and the responses were satisfactory.

Chapter 6

Results and discussion

After having described our model (Chapter 5), as well as the control strategy that we will use in our DC-DC converters (Chapter 4), we can now show the main outputs found from our simulations. Those results will be shown in the next three sections, focus on the generation units, storage unit and load side, respectively.

6.1 Generation units

As we discussed in the last chapter, one of the main parts of the model was the generation units and we are using two: PV and wind generations. As we saw in figures 5.3 and 5.5 their units have a maximum power point tracking (MPPT) algorithm associated with Boost converters in order to guarantee that both are working on their maximum power point (MPP). For both of them, we used the perturb and observe (P&O) algorithm, as described.

6.1.1 PV generation

For the PV generation we had two inputs: the irradiance of the installation site and its temperature. As expected, the irradiance played a major role in the output power produced by the PV panels, with and without the MPPT algorithm, and, for that reason, it is important to show the shape and amplitude of the site's irradiance:

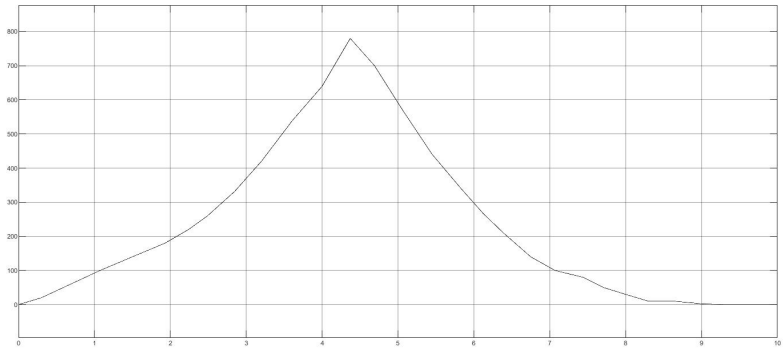

Figure 6.1: Irradiance of installation site (time (s) vs Irradiance ($\frac{W}{m^2}$))

As we can see, it assumes a peak value of around 800 $\frac{W}{m^2}$ in the middle of the period, which aimed at simulating the biggest irradiance of a given day, that happens around noon. As for the other input, the temperature, it's effect on the output power was shown in Figure 5.2, that is, for different temperatures, the MPP's voltage was slightly adjusted.

The first result that is important to show is the voltage, current and output power of the PV array in a scenario where we are not applying the MPPT algorithm to it. As we can see in the figure below, in this situation, the maximum output power is around 50 W at 4.3 seconds into the simulation and both the current and voltage were shaped as the irradiance.

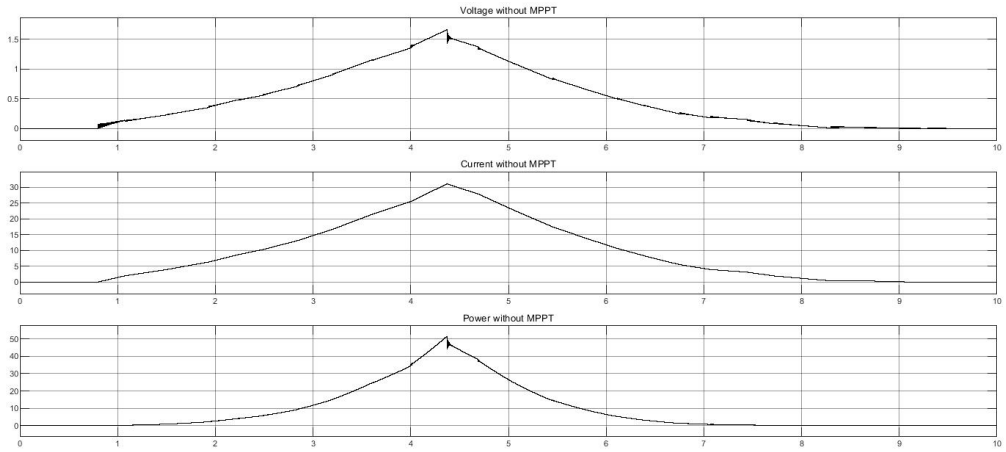

Figure 6.2: PV results without MPPT algorithm

Although the shape of the output power seems intuitively correct, as it should be strongly related to the irradiance, we know from Figure 5.2 that the MPP is

reached at a certain voltage level, dependent on the temperature, and therefore the voltage should not be shaped as the irradiance, in a ideal condition. From that same figure (5.2), it was clear that the voltage across the output terminals of the PV array should be between 25 to 35 V depending on the temperature, for the MPP to be reached and that was confirmed by the scenario where we used the MPPT algorithm in the PV array. As we can see in the figure below, the peak output power found in that scenario was significantly bigger (800 W at 4.3 seconds into the simulation).

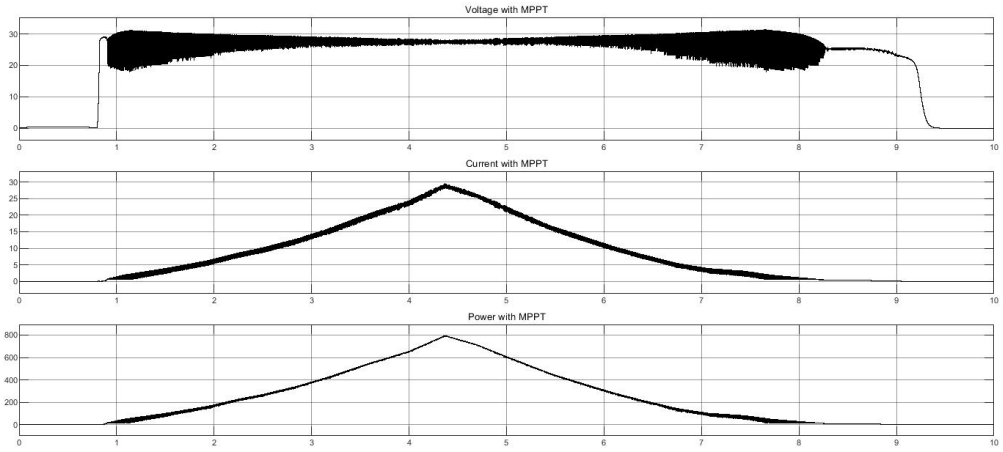

Figure 6.3: PV results with MPPT algorithm

The main difference, then, from the simulation with the MPPT algorithm and without it is the output voltage of the PV array. In this last scenario, with MPPT, the voltage was, for the majority of the simulation, kept at a level aroung 27V, attesting for the correct working of the tracking algorithm.

6.1.2 Wind generation

As for the wind generation, we have one important input, the the wind speed. As we can imagine, as it increases, the output power of the wind generation unit will increase as well, as we can see in Figure 6.4.

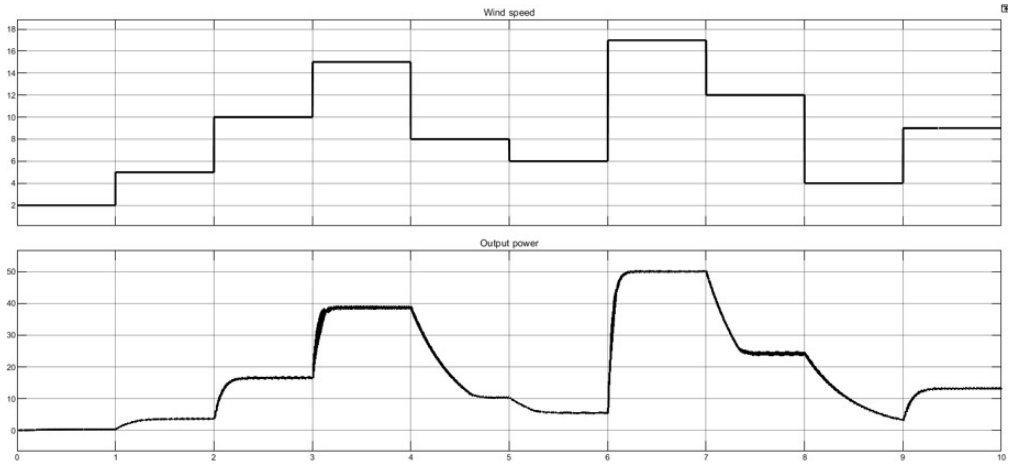

Figure 6.4: Wind results without MPPT algorithm

But, as mentioned in the description of the model, we have, as well here, a MPPT algorithm implemented in association with a Boost Converter, through the P&O strategy. As we can see comparing the next figure (with MPPT) with the previous one (without MPPT), the output power that we had was considerably increased, going from a peak of 50 W at a 17 $\frac{m}{s}$ wind speed to around 340 W at the same speed.

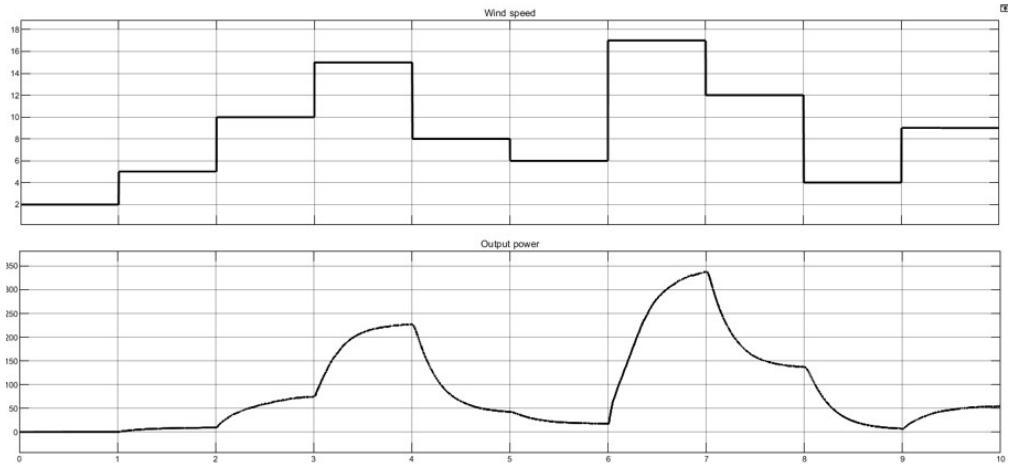

Figure 6.5: Wind results with MPPT algorithm

In conclusion, based on figures 6.5 and 6.3, we can attest for the importance of having well defined MPPT algorithms associated with the PV array and the wind turbines, in order to achieve a greater output power at our generation units.

6.2 Storage unit

Having shown the generation unit's results, we can now focus on the storage unit, that, as described, is made of bi-directional converters and batteries and has a main goal of setting a constant voltage level to a busbar, no matter the time on the simulation. This can be done because the battery can provide or absorb energy to or from the busbar, depending on the generation units providing less of more energy than the loads require. As mentioned before, we are dealing here with a bipolar DC Microgrid and, therefore, we will have three voltage levels available: $+V_{DC}$, $-V_{DC}$ and $+2.V_{DC}$.

In the figure below, we can attest the correct use of the storage unit, that is maintaining a steady voltage level at the main busbar, for all three voltage levels. It is important to mentioned that in our simulation V_{DC} is equal to 150 V.

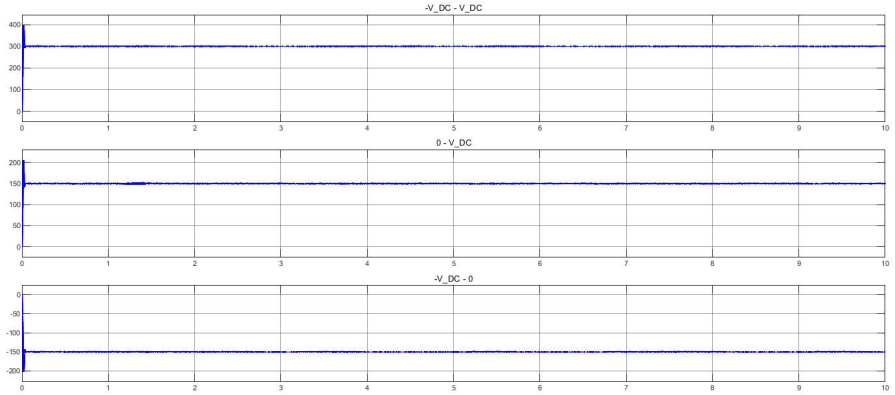

Figure 6.6: Voltage control in the main busbar

It is interesting to analyze, as well, the state of charge (SOC) of the battery, to see if, in our simulation, it is providing energy or absorbing it. From figures 6.5 and 6.3, we can see that the generation units are providing a maximum 350 W and 800 W, which is significantly smaller than the power needed to feed the loads (Table 5.5). That means that in our scenario, the battery would continuously provide energy to the system in order to guarantee the correct functioning of the system, which will make its SOC to decrease during the simulation. This can be seen in the figure below, where we see as well the irradiance, wind speed and voltage between the $+V_{DC}$ and $-V_{DC}$ wires (in red is the targeted value and in blue the actual measured value).

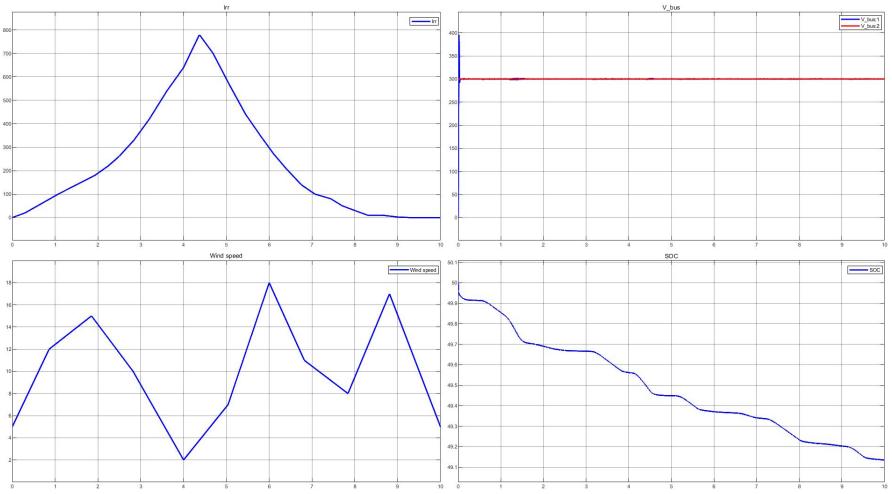

Figure 6.7: Storage unit results when battery discharging

From this simulation we can see that, although the main goal of the storage unit is being met, that is, maintaining the voltage levels of the main busbar steady in a reference value, the system is not sustainable, as the battery's SOC is only decreasing and will be, at some point, empty. That being said, in order to have a more sustainable Microgrid, we need to increase the amount of power provided from the generation units, which can be done by increasing the PV array area or adding more wind turbines to our wind generation unit. By doing this, we reached the situation provided below, where we can see that, throughout the simulation, the battery is absorbing more energy than providing it, which leads to its charging.

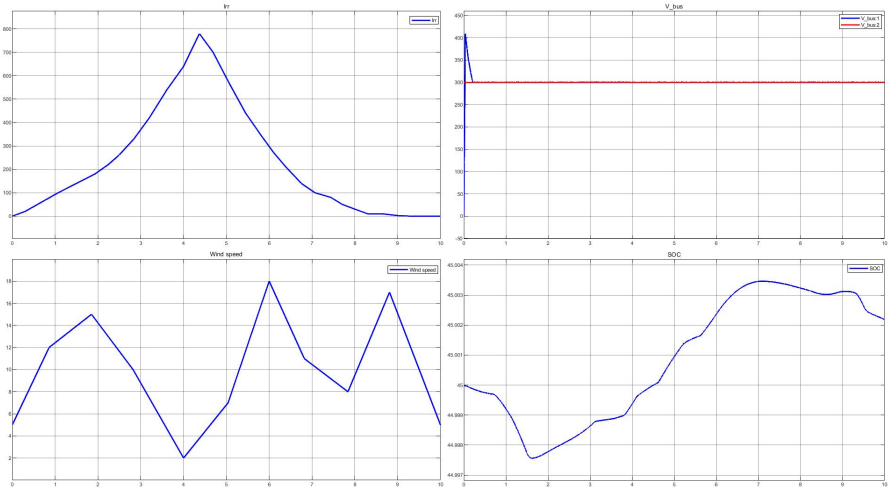

Figure 6.8: Storage unit results with increased generation capacity

As mentioned, this was possible by increasing the capacity of the generation units, done by increasing the PV panel's number of parallel string connected, from 5 to 500, which gave us a a peak power 100 times bigger than the one showed in Figure 6.3, that is 80.000W. As for the wind turbine, we increased the number of turbines that we had in our model, from one to fifty, and, therefore, we had a peak power 50 times bigger for the same wind speed, that is, for a $17\frac{m}{s}$ wind speed, we had 17.500W generated.

6.3 Load sides

Having discussed the generation and storage unit's results, we can jump to the loads. As mentioned in the description of the model, we have 5 groups of loads: 4 representations of houses, with several loads with different voltage levels and resistances and one high-voltage load. In all groups, the loads would be turned ON and OFF during the simulation and the control system would be in charge of regulating their voltage levels. In all simulations below, we can see in red the theoretical voltage level, going from zero to the voltage level described at Table 5.5 instantaneously and in blue we can see the actual measured value of the voltage across the loads.

Other than those voltage levels, we will show, as well, the voltage in the input of the houses, that is, after the transmission line and before the Boost converters used. This voltage would be related to the main busbar voltage shown in Figure 6.6, but not exactly with the same value because of the effect of the transmission line, as we will discuss below. The transmission lines lengths, resistances and inductances are shown in the table below.

Table 6.1: Transmission line parameters

Line	**Line lenght**	**Line resistance**	**Line inductance**
House 1	1000 m	0.073 Ω	0.92 mH
House 2	300 m	0.022 Ω	0.27 mH
House 3	900 m	0.066 Ω	0.83 mH
House 4	200 m	0.015 Ω	0.18 mH
High-voltage load	1000 m	0.073 Ω	0.92 mH

Once again, it is important to remember that between house 2 and the main busbar, we do not have only the transmission line related to house 2, but, as it is a secondary house, we have both the transmission line of house 1 and house 2 (Figure 5.13).

6.3.1 House 1

For the house 1, we simulated 5 different loads, two with low voltage levels, one with medium voltage level and two with high voltage levels. Their description is shown below.

Table 6.2: House 1 load parameters

Load	Voltage level (V)	Resistance (Ω)	Power (W)
Phone	20	100	4
Computer	40	200	8
Fridge	230	150	353
EV charger	450	3,6	52.250
Air-conditioner	400	80	2.000

As we can see from the table, the biggest load in terms of power is the EV charger and because of that we can anticipate that when this load is turned ON, the voltage in the input of the house will be smaller than the 150V at the main busbar. This can be understood by the fact that we would have a voltage divider consisting of the transmission line and the loads and, because the equivalent resistance of the loads at this moment would be much smaller, we would have a significant voltage drop in the transmission line. This can be seen in Figure 6.9, where, when we have the EV charger ON, the voltage in the input of the Boost converters are considerably smaller.

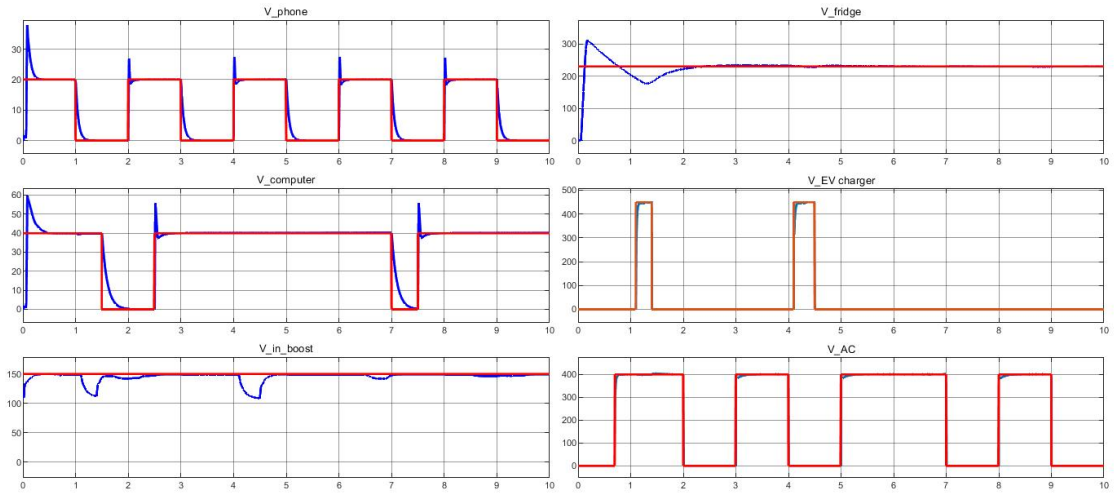

Figure 6.9: Voltage results for house 1

6.3.2 House 2

The loads of house 2 are shown in the table below.

Table 6.3: House 2 load parameters

Load	Voltage level (V)	Resistance (Ω)	Power (W)
Phone	30	130	7
Computer	50	180	14
Fridge	230	130	407
Shower	230	5,8	9.121
House heater	230	8,82	5.998

In the results of house 2, which we can see in Figure 6.10, it is clear the influence of the EV charger of house 1 on the input voltage of house 2. This happens because, as we saw on Figure 6.9, when the EV charger is turned ON, we have a voltage drop in the input of that house and, as house 2 shares that point of connection, it has an effect in here as well.

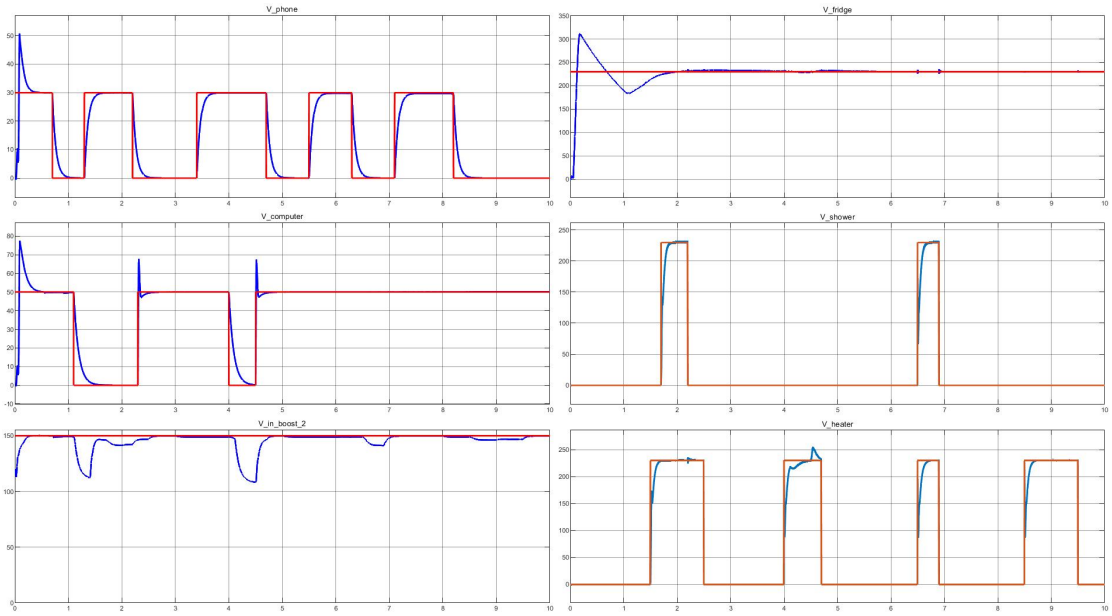

Figure 6.10: Voltage results for house 2

It is also clear that we have a voltage drop in the input of this house due to its own loads, specially the shower, as it is its biggest one. This effect of the shower could be seen on the input of house 1 as well (Figure 6.9), but it is, there, attenuated.

6.3.3 House 3

As for the house 3, again a primary house, but now connected between $-V_{DC}$ and the neutral line, we have fewer loads in this group, as we can see in the table below.

Table 6.4: House 3 load parameters

Load	Voltage level (V)	Resistance (Ω)	Power (W)
Phone	45	170	12
Computer	70	210	23
Fridge	230	100	529

As this house has only smaller loads, we can anticipate that its input voltage would suffer smaller variations. As we can see from Figure 6.11, house 3's loads are not major contributors to its input voltage variations, that exist due to house 4's loads, that shares the connection point of house 3 with it, as we can see in Figure 5.13.

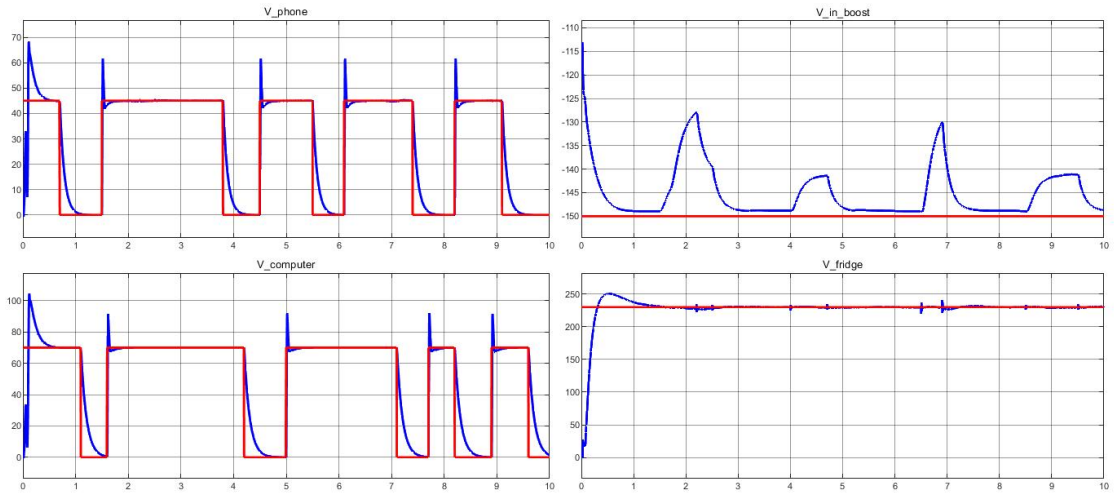

Figure 6.11: Voltage results for house 3

6.3.4 House 4

For the house 4, we have the following loads:

Table 6.5: House 4 load parameters

Load	Voltage level (V)	Resistance (Ω)	Power (W)
Phone	30	130	7
Computer	50	180	14
Fridge	230	130	407
Shower	230	5,8	9.121
Heater	230	8,82	5.998

In this house, we have, once again, bigger loads, such as a shower and a heater. For this reason, we will see a variation on the house's input voltage when they are turned ON and we will, as well, notice their effect on house 3, as mentioned above and seen in figure 6.11. As we analyze the amplitude of the input voltage's variations on both houses, it is clear that the effect on house 3 is smaller (around 20V there and 25V here) and this can be understood by the presence of a transmission line, that attenuates the voltage drop transmitted upwards in the model.

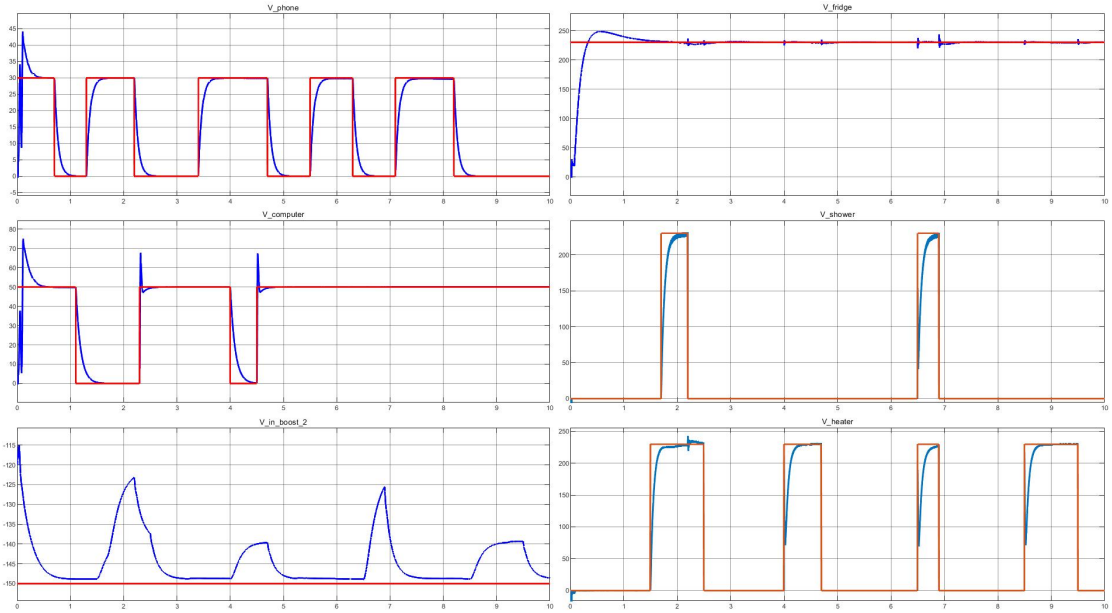

Figure 6.12: Voltage results for house 4

6.3.5 High voltage site

Finally, for the high voltage site, the one that is connected between $-V_{DC}$ and V_{DC} in the main busbar, which in our case corresponds to 300V, we have one load with a voltage level of 650V and resistance of 5,8 Ω. Its results can be found in the figure below:

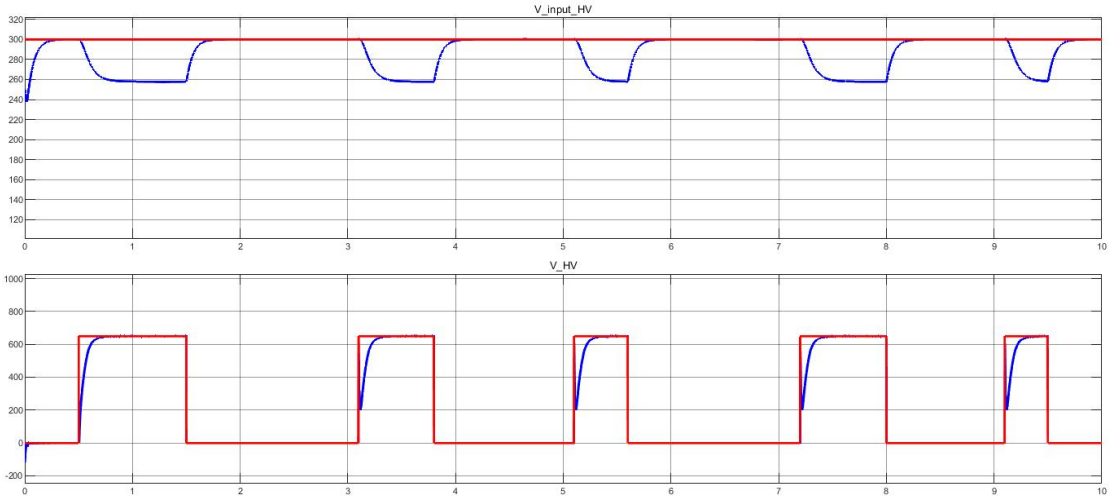

Figure 6.13: Voltage result for HV load

6.4 Discussion of results

From this chapter we could see the main results of the simulations made on MATLAB/ Simulink. We discussed the importance of having some well defined MPPT algorithm when using PV and wind generation units, as shown in figures 6.3 and 6.5. By using the P&O algorithm, we were able to increase the power provided to the microgrid, even maintaining the parameters of the panels and turbines.

Also, we provided some results that proven the importance of having a storage unit that would, not only maintain a steady voltage on the main busbar, as shown in Figure 6.6, but guarantee that our loads are fed with the necessary power, no matter the weather conditions. As we saw, one important variable to check on isolated microgrids is the state-of-charge (SOC) of the batteries that we are using, as it cannot only reduce in our simulation, as seen in Figure 6.7, because this would mean that we are not providing enough energy for our system to work continuously. If that happens, we need to increase our generation capacity, until the net result of the battery's SOC is positive, as seen in Figure 6.8.

During the discussion, we also highlighted the variations that we had in the input of the houses due to the turning ON and OFF of big loads, such as the EV charger. Although these variations are in some cases considerable, changing the voltage level up to 30% of its value, it is important to understand that this is not a problem, because, in our model, we did not intend nor try to control that specific voltage level.

Our goal was to control the main busbar's voltage, for all three voltage levels of our bipolar microgrid and, as we shown in Figure 6.6, this was done perfectly. Also, it was important to control the voltage levels on the loads side, that is, where the computers, phones, air-conditioners and all other loads were connected. As we showed in figures 6.9, 6.10, 6.11, 6.12 and 6.13, the controlling of those voltage levels worked properly, having fast responses and being able to maintain the voltage steady at the reference given, proving right, then, the control strategy defined on Chapter 4.

In this chapter, we also gave attention to the propagation of voltage oscillations within the microgrid, that is, how the turning ON and OFF of one house's load would affect another house's voltage level. From the discussions and results shown, it was clear that we do have an effect on the house's input voltage level when we turned ON and OFF the loads of another house, but only if they were neighbour houses, that is, only if they shared one transmission line (house 1 and 2 or house 3 and 4). This effect, on the other hand, was a little attenuated by the transmission line between the houses, as we would have, on themselves, a voltage drop. For the other loads, the ones that only shared the main busbar as a point of common coupling (PCC), the propagation of their effect was not seen, because, as we saw in Figure 6.6, the voltage on the main busbar kept steady during our simulations.

It is important to mention that, even having several loads with different sizes being turned ON and OFF at different moment in the simulations, the voltage levels at the load side were correctly controlled. The strategy to use first a Boost Converter, from the transmission line to the house, then, in series with it, a Buck converter in order to obtain smaller voltage levels, proved right and even in these scenarios, the response was almost instantaneous. The association in series, then, of DC-DC converters was not a problem in our simulation, but a solution to the problem of considering the transmission line when setting the control parameters. The implementation of transmission lines into Boost converters showed to be easy to control, as we would, in our calculation, just add in series a pair of inductor and resistance in our model.

Chapter 7

Conclusion

This thesis aimed at providing a technologically viable grid approach that allows the substitution of fossil fuel sources for RES. During this work, we have shown that these sources are economically viable nowadays and can even have smaller LCOE compared to the others, what disproves the illusion that many people have that RES are expensive and, therefore, not a possible alternative.

In order to guarantee the best use of these sources, we argued in favour of Isolated DC Microgrids for their implementation, based on two main arguments. First, that it is a nice solution to the transmission losses problem, very significant in centralized distribution grid approaches, such as the ones that we have today. And second, that, nowadays, DC transmission grids are more viable as we have a growing share of those kinds of loads and, by avoiding AC-DC conversions, we could reduce losses and increase the grid's efficiency. Based on those two arguments, we were able to shift the paradigm of centralized AC grids towards DC microgrids.

Having decided to study DC microgrids in our thesis, we had to focus our attention on some very important devices: DC-DC converters. Their role is essential as they are in charge of adjusting voltage levels at different points of our grid, which is necessary as generation units and loads can operate on different voltage levels. Due to this importance, the first thing that we had to do was a thorough study on the main types of converters that are available in the market and, in here, we divided them in two groups: the non-isolated ones and the isolated ones.

As we saw in chapters 2 and 3, the main difference between these two types is the presence of a transformer in the later group. This transformer brought a major safety advantage to these converters as it provides isolation, which means that no current flows from their primary to secondary side. Although this is important, transformers bring, as well, a major setback to isolated converters: their losses,

which leads to major efficiency reductions to the converters that had them. It was based on their efficiencies that we decided to use Buck and Boost converters in our model, as with them we could step down and up the voltage levels in our model, with reduced losses.

Having decided for these converters, we had, then, to look for a way to control their output voltage levels in a way that was easily adjustable to different loads and different input voltages and that shown a fast and stable response. In Chapter 4, we discussed a mathematical approach to set all four control parameters (proportional and integral of both the current and voltage loops), in which we would pre-define the time constants ($\tau_{current}$ and $\tau_{voltage}$) of a first order transfer function for both loops and, based on those values, set their control parameters.

As we shown, there was only one combination of control parameters' values that would allow us to have a first order response for that loop. It is important to mention that, by using this approach, we could guarantee that the inner loop's response was much faster than the outer loop's one, which was a requirement for the proper working of cascade controllers. Finally, as we showed, the control parameters would just be dependent on the converter parameters and the defined time constants, which made it easy to adapt to different scenarios, as we aimed at.

After defining a control strategy, we could start developing a model of a DC Microgrid to put this and other concepts into practice. In this model, described in Chapter 5, we used only RES (PV and wind generation), with specific MPPT algorithms associated with them. We also developed a storage unit for our microgrid, as we need to guarantee that, even when the generations units are not providing enough power, due to weather condition, the loads are fed with necessary energy to work properly. The way that we did this was by associating a battery with a bidirectional DC-DC converter, with a specific control, in order to feed the loads with power when the generation units were not able to do so and, therefore, discharging the battery, and absorb energy from the generation units when they were providing more than the loads required. By doing this, we were able to guarantee, as well, steady voltage levels on the main busbar of the grid and, as we developed a bipolar DC microgrid, we provided at that busbar not only one voltage level, but three (V_{DC}, $-V_{DC}$ and $2V_{DC}$), thus increasing the system's flexibility and allowing the provision of power even in fault scenarios.

At the load end, we decided to organize them in several groups, each containing different loads that required different voltage levels and load powers, simulating consumer houses, with every-day's electrical devices, such as computers, phones,

showers and others. Each of these loads would be connected and disconnected throughout the simulations and the control strategy developed would be in charge of controlling their voltages. We simulated as well, with these houses, the effect of having DC-DC controllers in series and in parallel with each other, in order to provide an extensive discussion about it.

In the Chapter 6, we shown all the results from our simulations, which proved the control approach defined right. In all loads, from small ones, such as computers, to big ones, such as EV chargers, the control system showed a rapid response and was able to keep the voltage levels steady in their reference value, with very little oscillation. Even the effect of one load in another, through series or parallel converters, were considerably reduced, all being within 5% of voltage variation from the action of one load being turned ON of OFF in another one. At the end, what we could see in all house examples, as well as in the high-voltage load, was a variation in the input voltage of the houses, that is, before the Boost Converter that connected the transmission line to the loads, but not on the load side or on the main busbar, which was the goal of our simulation.

Based on the results presented, we believe that the goal of this thesis, which was to provide a grid architecture able to be fed only by RES, was perfectly met. We developed an Isolated DC Microgrid, with only PV and wind sources of energy, that was not only reliable but efficient. In our simulations, we implemented a real life scheme of this microgrid, taking into account transmission lines, several loads with different characteristics and requirements working in parallel, real weather inputs and real battery models, and, even for this complex scenario, the response that we had on the load side not only converged to correct value set, but were very fast in doing that. Due to this, we believe that this thesis can be understood as a big argument in favour of the implementation of Isolated DC Microgrids and may, one day, affect the way that we see our energy grids.

7.1 Future work

Although this study already showed some interesting results, there are still some opportunities for improvement. As we discussed in Chapter 5, in order to model a DC microgrid that is as close to reality as possible, we implemented some transmission lines between the main busbar and the loads and between groups of loads. On the other hand, the generation units and the storage unit were connected in the same physical point, without any transmission line between them, what, in reality, is not true. For this reason, it is clear that the one model improvement that we could do would be to implement this transmission line.

In the same Chapter 5, we showed that the power converters linked to the loads were controlled based on the approach described in Chapter 4, but the same cannot be said about the power converter of the storage unit, with was controlled by two PI controllers with pre-defined control parameters, as shown in figure 5.7. Those control parameters were found by trial and error and, therefore, are not optimal. A control strategy for it would be an interesting improvement of the described model.

One strategy that we used in this thesis was to connect the transmission lines to the houses by only Boost converters, as we could easily add the contribution of the line to the converter without changing its mathematical model described in Chapter 4. Although this strategy was proven right and, when needed we just connected a Buck Converter in series with the Boost one, in order to feed the loads, it would be interesting to add the transmission line contribution to the Buck Converter and understand how this would change the model described in Equation 4.3 and how this would affect the control parameters found for that converter.

Finally, as we mentioned during this work, a microgrid's energy reliability increases as we have more diverse sources and, with that in mind, our model used not only one RES, but two: PV and wind energy. Although this shows already some interesting results, we could increase the number of sources that we have in order to avoid problems due to weather fluctuations and, therefore, we could implement other RES in our model, such as, for example, fuel cells.

Bibliography

[1] European Comission. *Forging a climate-resilient Europe - the new EU Strategy on Adaptation to Climate Change*. https://ec.europa.eu/clima/sites/clima/files/adaptation/what/docs/eu_strategy_2021.pdf/. 2021.

[2] White House. *President Biden Sets 2030 Greenhouse Gas Pollution Reduction Target Aimed at Creating Good-Paying Union Jobs and Securing U.S. Leadership on Clean Energy Technologies*. https://www.whitehouse.gov/briefing-room/statements-releases/2021/04/22/fact-sheet-president-biden-sets-2030-greenhouse-gas-pollution-reduction-target-aimed-at-creating-good-paying-union-jobs-and-securing-u-s-leadership-on-clean-energy-technologies/. 2021.

[3] United States Environmental Protection Agency. *Source of Greenhouse Gas Emissions*. https://www.epa.gov/ghgemissions/sources-greenhouse-gas-emissions/. 2020.

[4] Michaja Pehl et al. "Understanding future emissions from low-carbon power systems by integration of life-cycle assessment and integrated energy modelling". In: *Nature Energy* 2.12 (2017), pp. 939–945.

[5] IEA. *Evolution of solar PV module cost by data source, 1970-2020*. https://www.iea.org/data-and-statistics/charts/evolution-of-solar-pv-module-cost-by-data-source-1970-2020/. 2020.

[6] Pietro Tumino. *Understanding the Difference Between Distributed and Centralized Generation*. https://eepower.com/technical-articles/understanding-the-difference-between-distributed-and-centralized-generation/. 2021.

[7] L. E. Zubieta and P. W. Lehn. "A high efficiency unidirectional DC/DC converter for integrating distributed resources into DC microgrids". In: *2015 IEEE First International Conference on DC Microgrids (ICDCM)*. 2015, pp. 280–284. DOI: 10.1109/ICDCM.2015.7152054.

[8] Strategic Microgrid. *About Microgrids*. https://strategicmicrogrid.com/about-microgrids/. 2019.

[9] Robert W Erickson. "DC–DC power converters". In: *Wiley encyclopedia of electrical and electronics engineering* (2001).

[10] Douglas R. Danley. *Defining a Microgrid Using IEEE 2030.7*. https://www.cooperative.com/programs-services/bts/Documents/TechSurveillance/Surveillance-Defining-Microgrids-November-2019.pdf/. 2019.

[11] Derrick Magdefrau et al. "Analysis and review of DC microgrid implementations". In: *2016 International Seminar on Application for Technology of Information and Communication (ISemantic)*. IEEE. 2016, pp. 241–246.

[12] Jeremi Martin. "Distributed vs. centralized electricity generation: are we witnessing a change of paradigm". In: *An introduction to distributed generation* (2009).

[13] Anand Patwardhan et al. "Transitions in Energy Systems. Chapter 16". In: Jan. 2012.

[14] Lazard. *Lazard's Levelized Cost of Energy ("LCOE") analysis*. https://www.lazard.com/media/451086/lazards-levelized-cost-of-energy-version-130-vf.pdf. 2019.

[15] Robert R. Nordhaus Paul Savage and Sean P. Jamieson. "DC Microgrids: Bene[U+FB01]ts and Barriers". In: *yale school of forestry environmental studies* (), pp. 51–66.

[16] Shengwen Li et al. "A Comparison of Energy Efficiency in AC and DC Microgrid with New Energy". In: *IOP Conference Series: Earth and Environmental Science*. Vol. 619. 1. IOP Publishing. 2020, p. 012057.

[17] River Glennapts. *Buck Converter | Step Down Chopper*. https://riverglennapts.com/nl/converters/213-buck-converter-step-down-chopper.html. 2019.

[18] Marc Bekemans. *2. DC-DC Converter*. 2020.

[19] ON Semiconductor. "Buck Converter External Components Selection". In: (2017).

[20] Saurabh Kumar, Rajat Kumar, and Dr. Navdeep Singh. "Performance of closed loop SEPIC converter with DC-DC converter for solar energy system". In: Mar. 2017. DOI: 10.1109/ICPCES.2017.8117668.

[21] River Glennapts. *Buck Boost Converter*. https://riverglennapts.com/nl/converters/216-buck-boost-converter.html. 2019.

[22] Hengyang Luo, Huiqing Wen, and Xingshuo li. "Distributed MPPT control under partial shading condition". In: May 2016, pp. 928–932. DOI: 10.1109/IPEMC.2016.7512411.

[23] Paul Mitcheson and Tzern Toh. “Power management electronics”. In: *Energy Harvesting for Autonomous Systems* (Jan. 2010), pp. 1–57.

[24] Ron Stull. *Isolated vs Non-Isolated Power Converters*. https://www.cui.com/blog/isolated-vs-non-isolated-power-converters/. 2019.

[25] Steven Keeping. “Use Isolated DC-DC Converters with Embedded Transformers to Ease Assembly”. In: (2020).

[26] Steven Keeping. *Use Isolated DC-DC Converters with Embedded Transformers to Ease Assembly*. https://www.digikey.com/en/articles/use-isolated-dc-dc-converters-with-embedded-transformers-to-ease-assembly/. 2020.

[27] Unal Yilmaz et al. “Investigation of Closed-Loop Controlled Isolated DC-DC Converters with HighFrequency Transformers”. In: Nov. 2017.

[28] Mohammed Abdul Khader Aziz Biabani. “Simulation, mathematical calculation and comparison of power factor and efficiency for forward, fly back and proposed forward-flyback converter”. In: *2016 International Conference on Electrical, Electronics, and Optimization Techniques (ICEEOT)*. 2016, pp. 1583–1589. DOI: 10.1109/ICEEOT.2016.7754952.

[29] KingCreate Instruments. *What is the difference between on/off control and PID control ?* http://www.kcmeter.com/servicesread.asp?id=11. 2018.

[30] EL-PRO-CUS. *What is a PID Controller : Working Its Applications*. https://www.elprocus.com/the-working-of-a-pid-controller/. 2020.

[31] Afarulrazi Bakar et al. “DC/DC boost converter with PI controller using Real-Time Interface”. In: 10 (Jan. 2015), pp. 9078–9082.

[32] DEWEsoft. *PID Control*. https://training.dewesoft.com/online/course/pid-control. 2020.

[33] Remon Das, Humayun Rashid, and Iftekhar Uddin Ahmed. “A comparative analysis of PI and PID controlled bidirectional DC-DC converter with conventional bidirectional DC-DC converter”. In: *2017 3rd International Conference on Electrical Information and Communication Technology (EICT)*. 2017, pp. 1–6. DOI: 10.1109/EICT.2017.8275149.

[34] Santanu Kapat and Philip T. Krein. “Formulation of PID Control for DC–DC Converters Based on Capacitor Current: A Geometric Context”. In: *IEEE Transactions on Power Electronics* 27.3 (2012), pp. 1424–1432. DOI: 10.1109/TPEL.2011.2164423.

[35] Ounis Rabiaa et al. “Cascade Control Loop of DC-DC Boost Converter Using PI Controller”. In: *2018 International Symposium on Advanced Electrical and Communication Technologies (ISAECT)*. 2018, pp. 1–5. DOI: 10.1109/ISAECT.2018.8618859.

[36] PE Vance Vandoren PhD. *Fundamentals of cascade control*. https://www.controleng.com/articles/fundamentals-of-cascade-control/. 2014.

[37] Konstantinos F. Krommydas and Antonio T. Alexandridis. “Nonlinear design and stability analysis with experimental validation of cascaded pi controlled dc/dc boost converters”. In: *2015 54th IEEE Conference on Decision and Control (CDC)*. 2015, pp. 5043–5048. DOI: 10.1109/CDC.2015.7403008.

[38] Dinesh Kumar, Firuz Zare, and Arindam Ghosh. “DC Microgrid Technology: System Architectures, AC Grid Interfaces, Grounding Schemes, Power Quality, Communication Networks, Applications and Standardizations Aspects”. In: *IEEE Access* PP (Apr. 2017), pp. 1–1. DOI: 10.1109/ACCESS.2017.2705914.

[39] European comission. *PHOTOVOLTAIC GEOGRAPHICAL INFORMATION SYSTEM*. https://re.jrc.ec.europa.eu/pvg_tools/en/tools.html. 2020.

[40] Weather Spark. *Average Weather in Louvain-la-Neuve*. https://weatherspark.com/y/51061/Average-Weather-in-Louvain-la-Neuve-Belgium-Year-Round. 2020.

[41] Sony Venugopal, Akshay Aspalli, and R. Raveendra. “Maximum Power Point Tracking For Photovoltaic Systems”. In: Jan. 2017, pp. 432–441. DOI: 10.21647/ICCTEST/2017/49002.

[42] Lazarus Stefan and Feri Yusivar. “Modeling of Wind Turbine Generator with Boost Converter MPPT”. In: *2018 2nd International Conference on Smart Grid and Smart Cities (ICSGSC)*. 2018, pp. 100–104. DOI: 10.1109/ICSGSC.2018.8541306.

[43] Manuel Reta-Hernández. “Transmission line parameters”. In: *Electric Power Generation, Transmission, and Distribution: The Electric Power Engineering Handbook*. CRC Press, 2018, pp. 14–1.

UNIVERSITÉ CATHOLIQUE DE LOUVAIN
École polytechnique de Louvain
Rue Archimède, 1 bte L6.11.01, 1348 Louvain-la-Neuve, Belgique | **www.uclouvain.be/epl**